Monsoons


MAZDA

Mean January 200 hPa Divergent Wind,

Outgoing Longwave Radiation

1979-2001

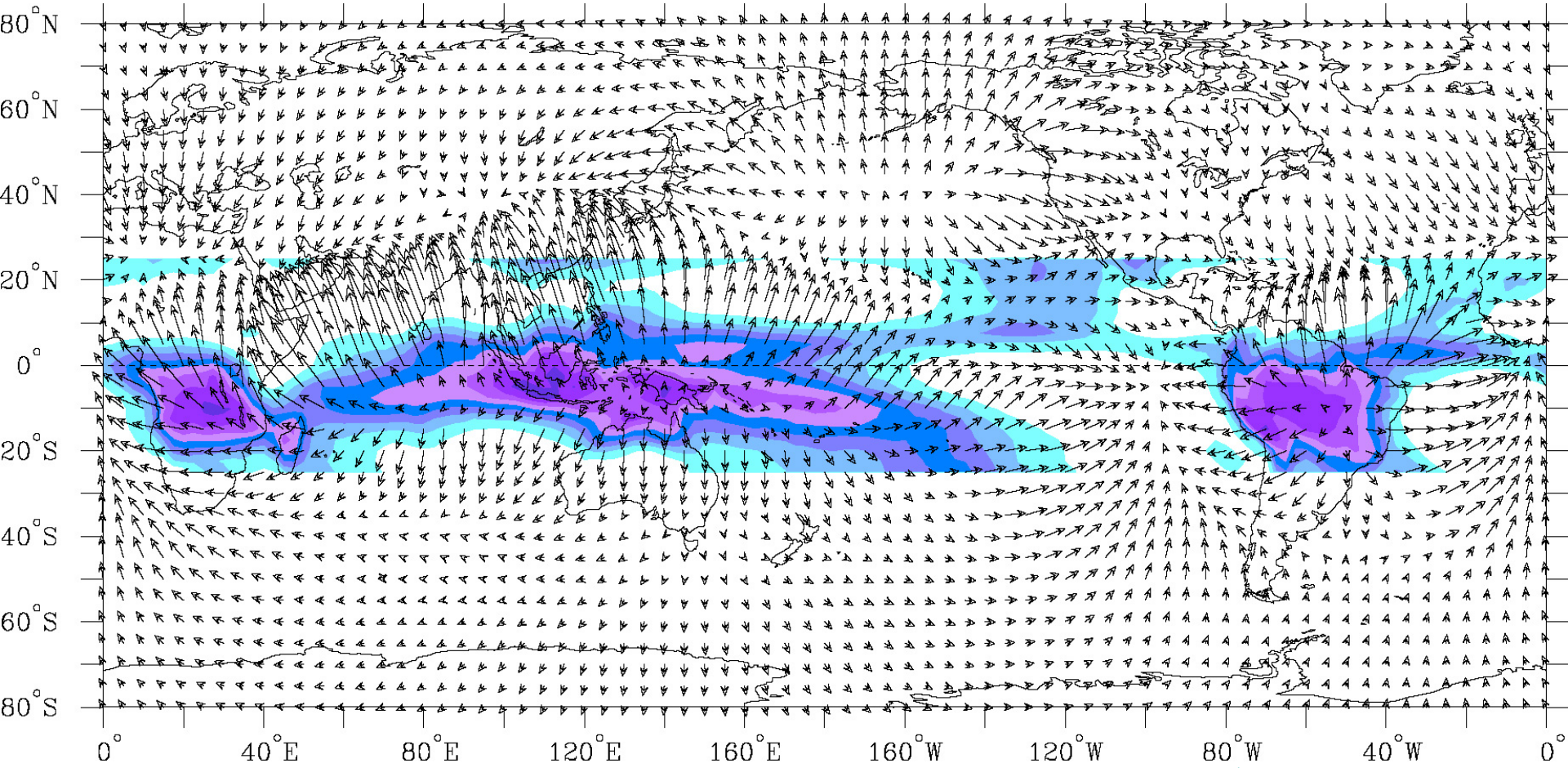

Div. Wind (vectors, largest around 15 m s^{-1})

OLR (shading at 10 W s^{-2} intervals)

Mean July 200 hPa Divergent Wind,

Outgoing Longwave Radiation

1979-2001

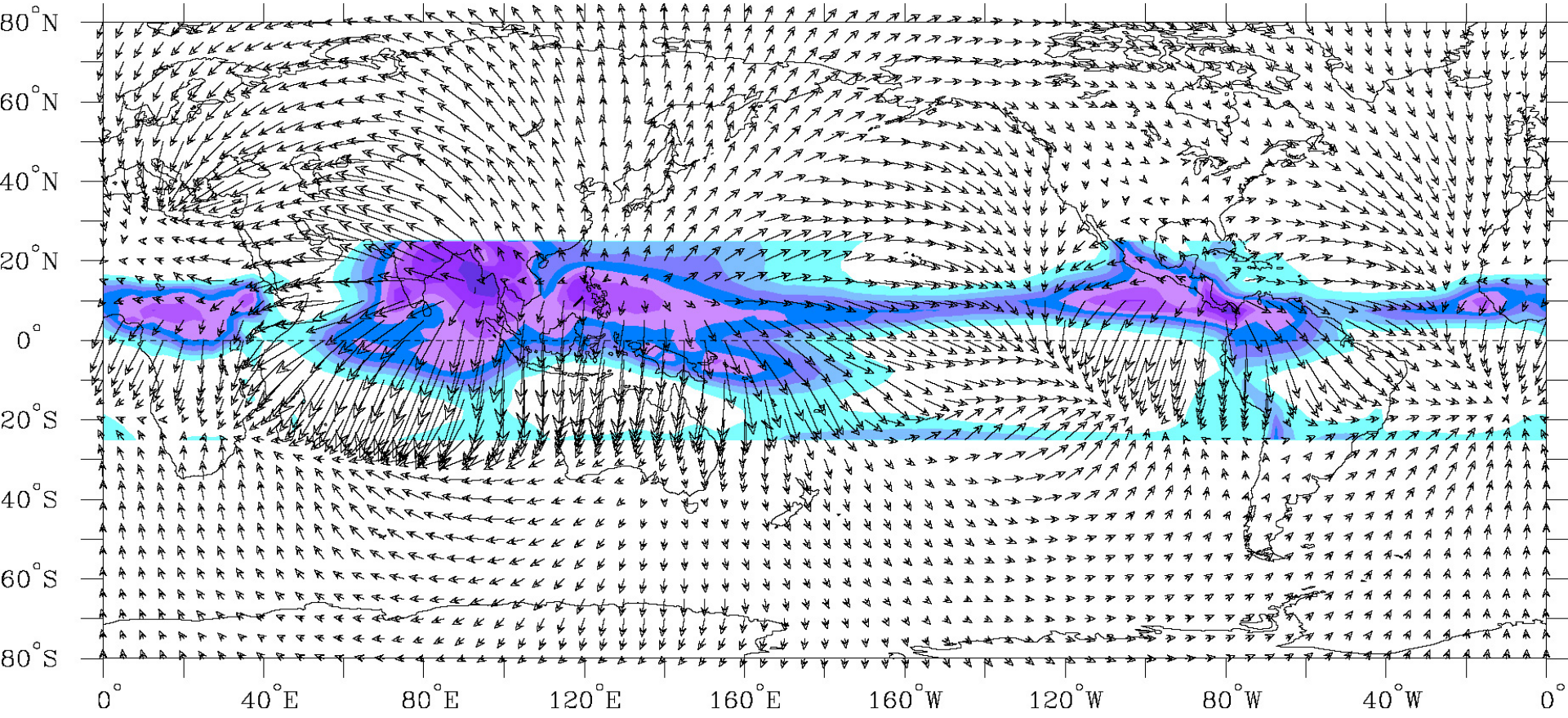

Div. Wind (vectors, largest around 15 m s^{-1})

OLR (shading at 10 W s^{-2} intervals)

Observed Zonal Mean Monsoon Flow

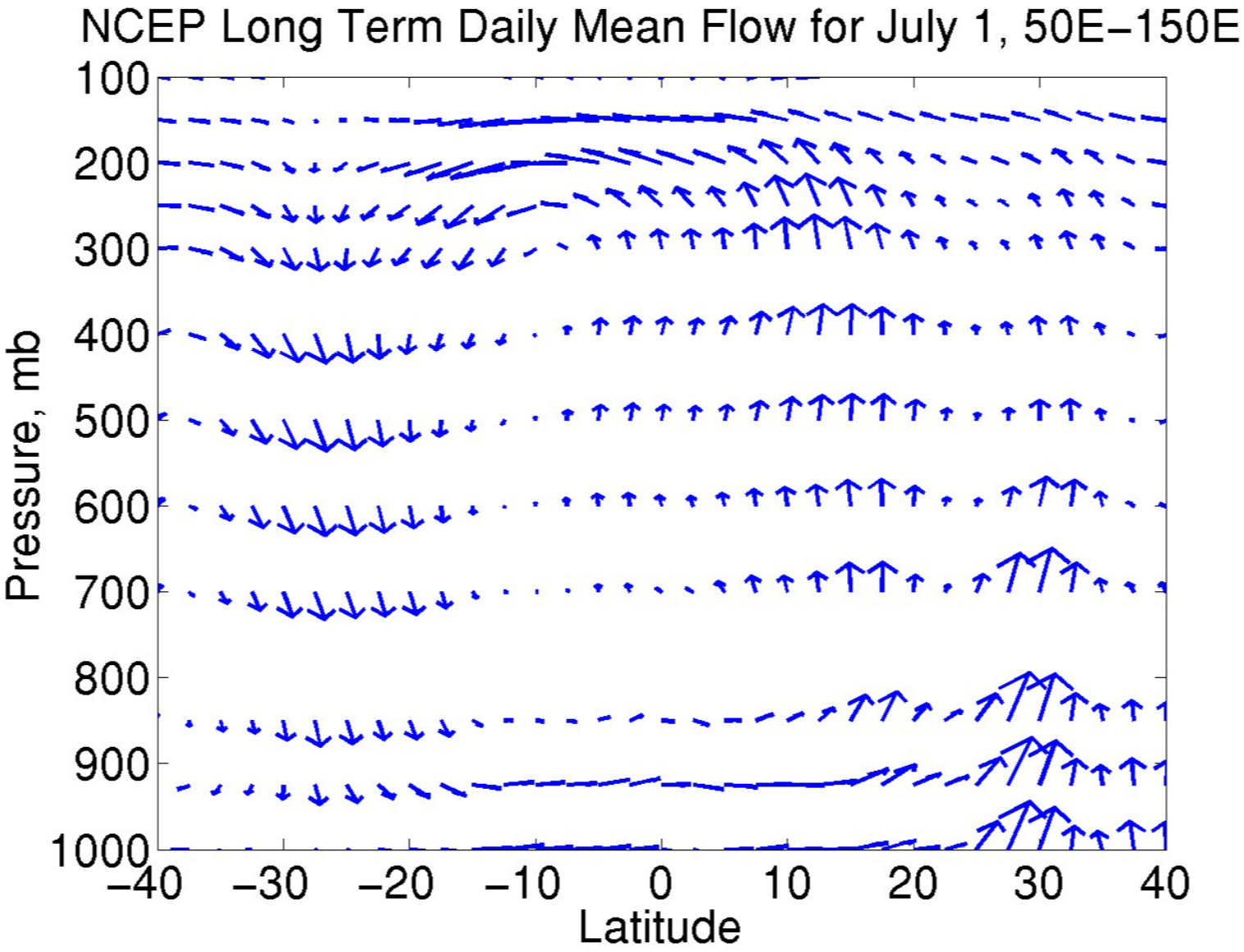

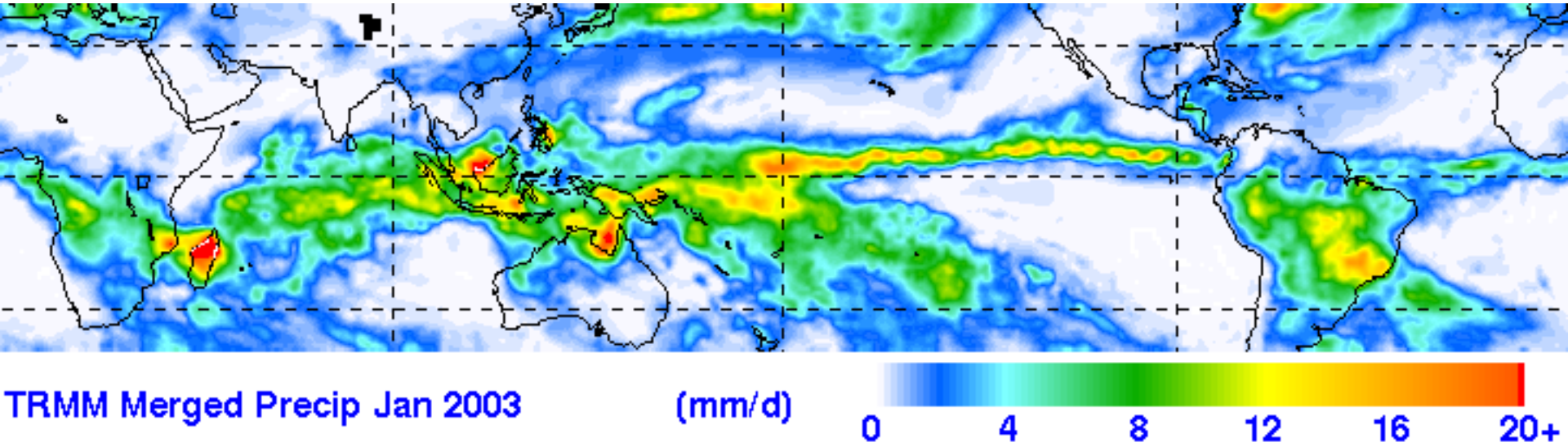
TRMM Merged Precip Jan 2003
(mm/d)
0
4
8
12
16
20+

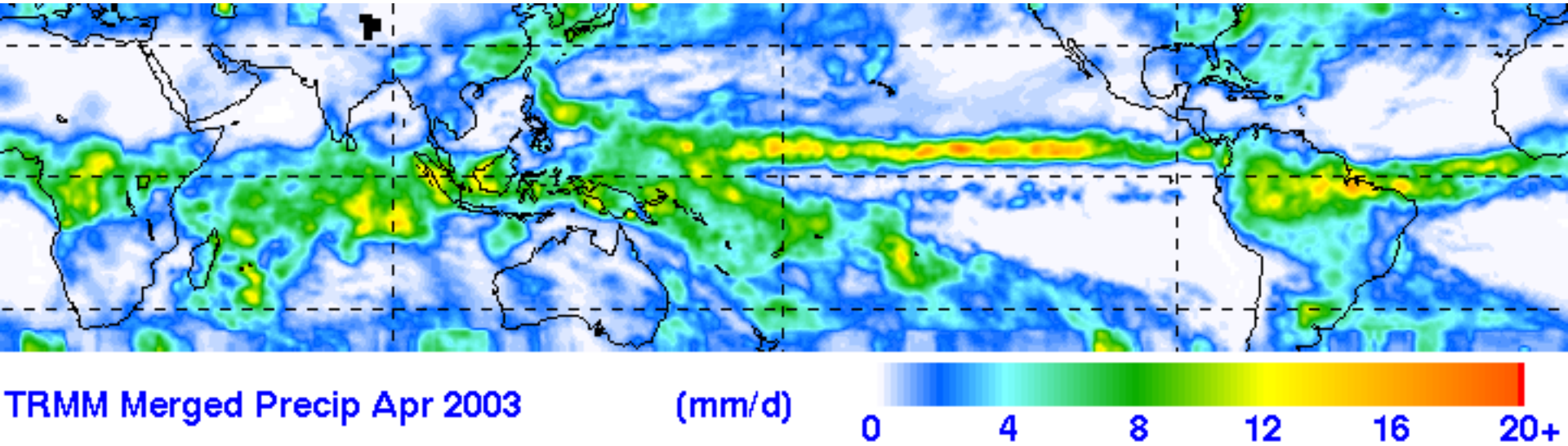
TRMM Merged Precip Apr 2003
(mm/d)
0
4
8
12
16
20+

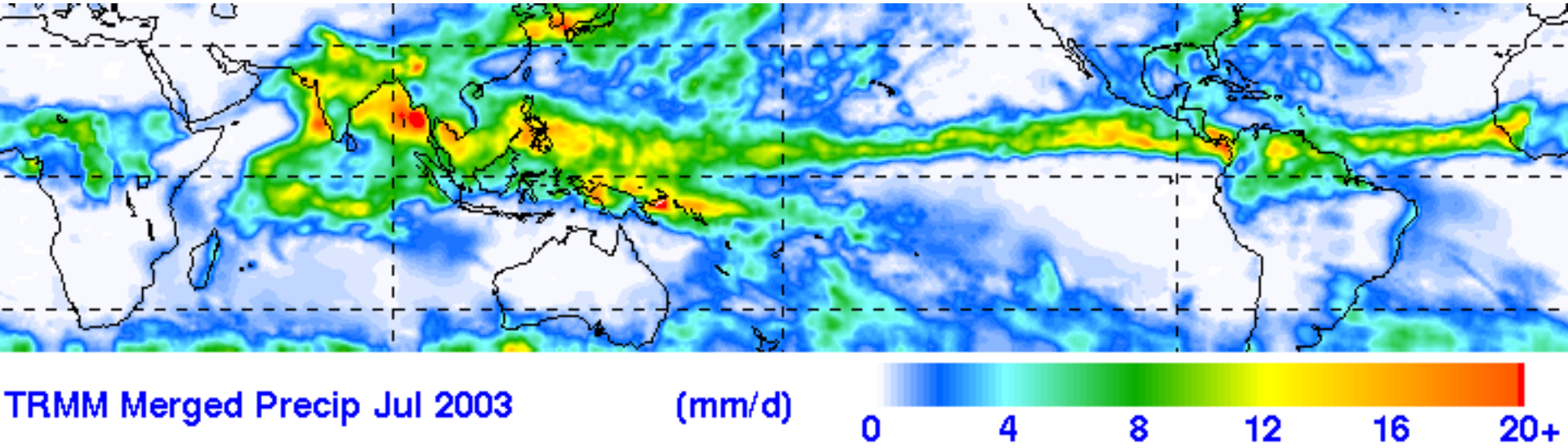
TRMM Merged Precip Jul 2003
(mm/d)
0
4
8
12
16
20+

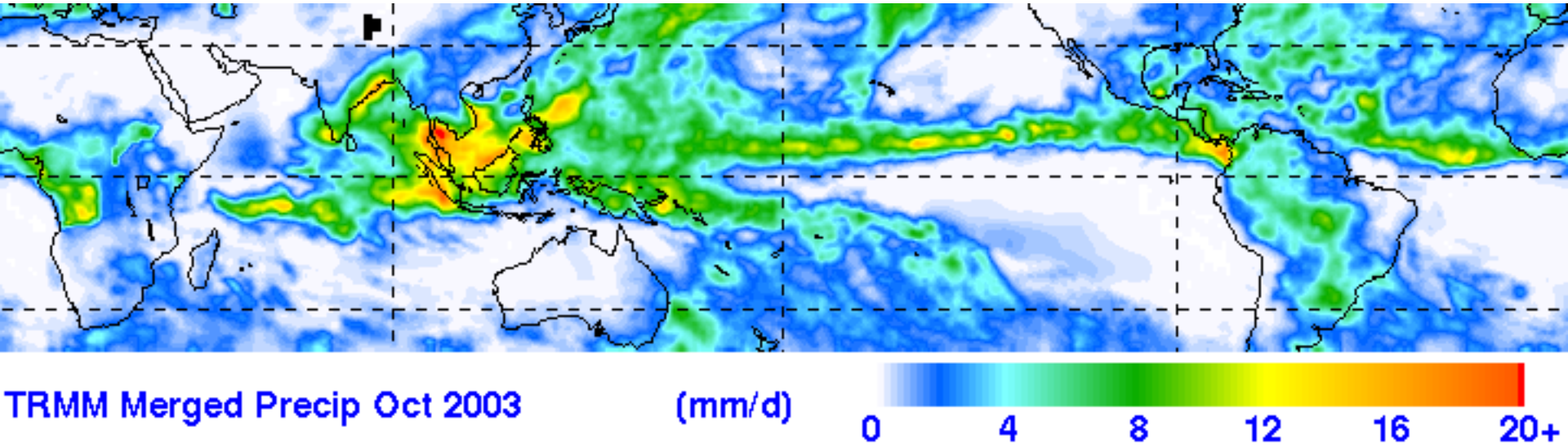
TRMM Merged Precip Oct 2003
(mm/d)
0
4
8
12
16
20+

250 hPa heights, 15 January 1995

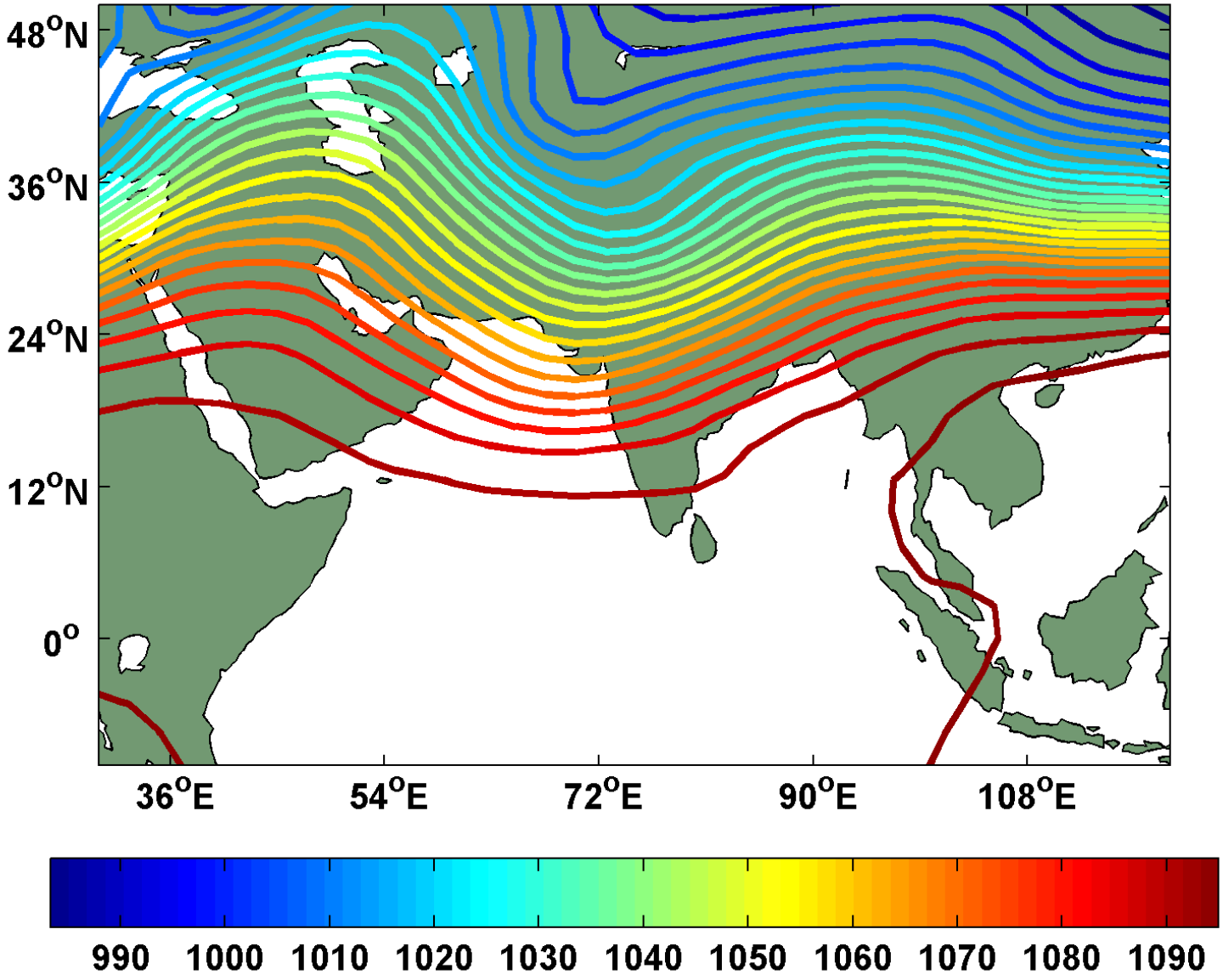

250 hPa heights, 15 July 1995

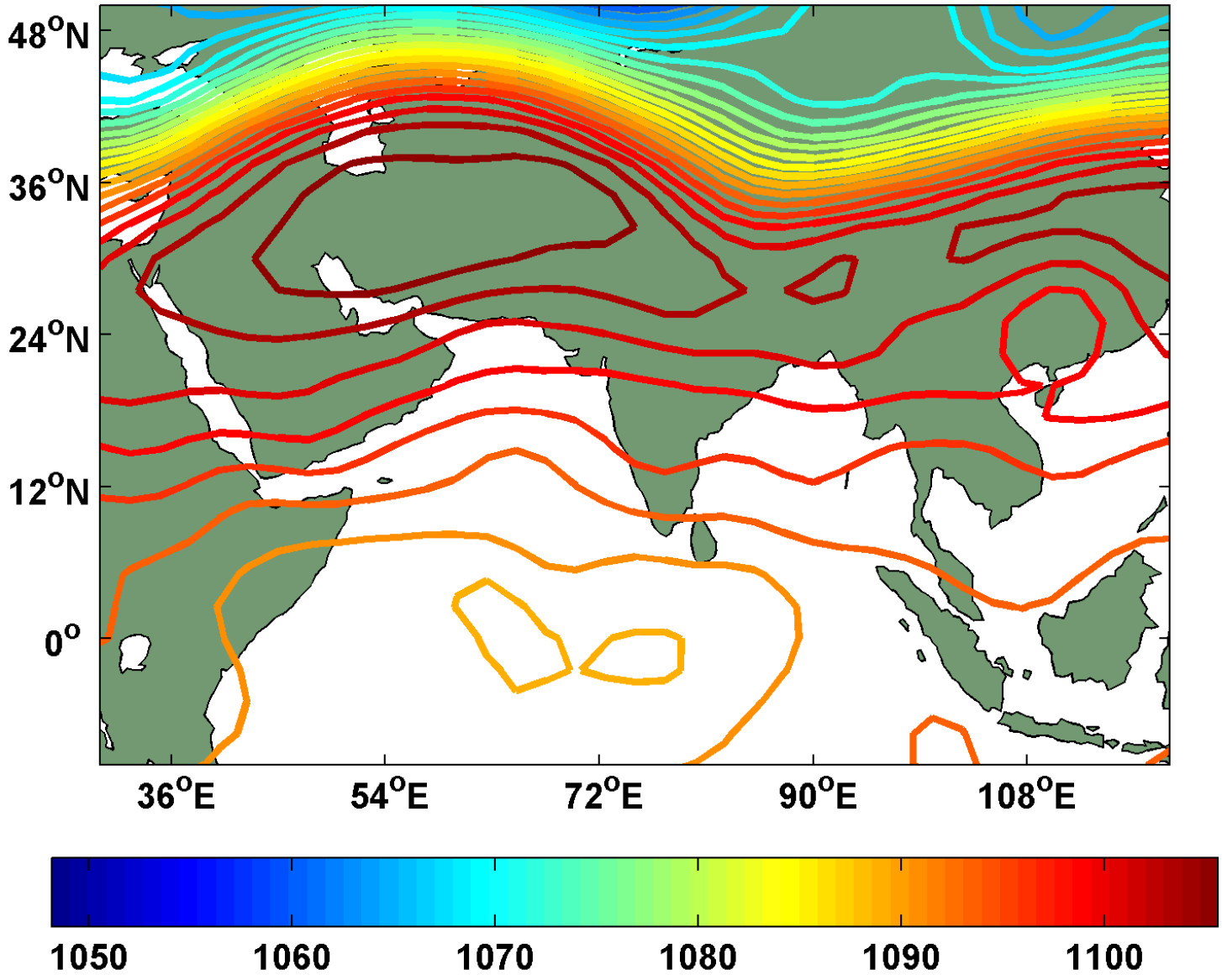

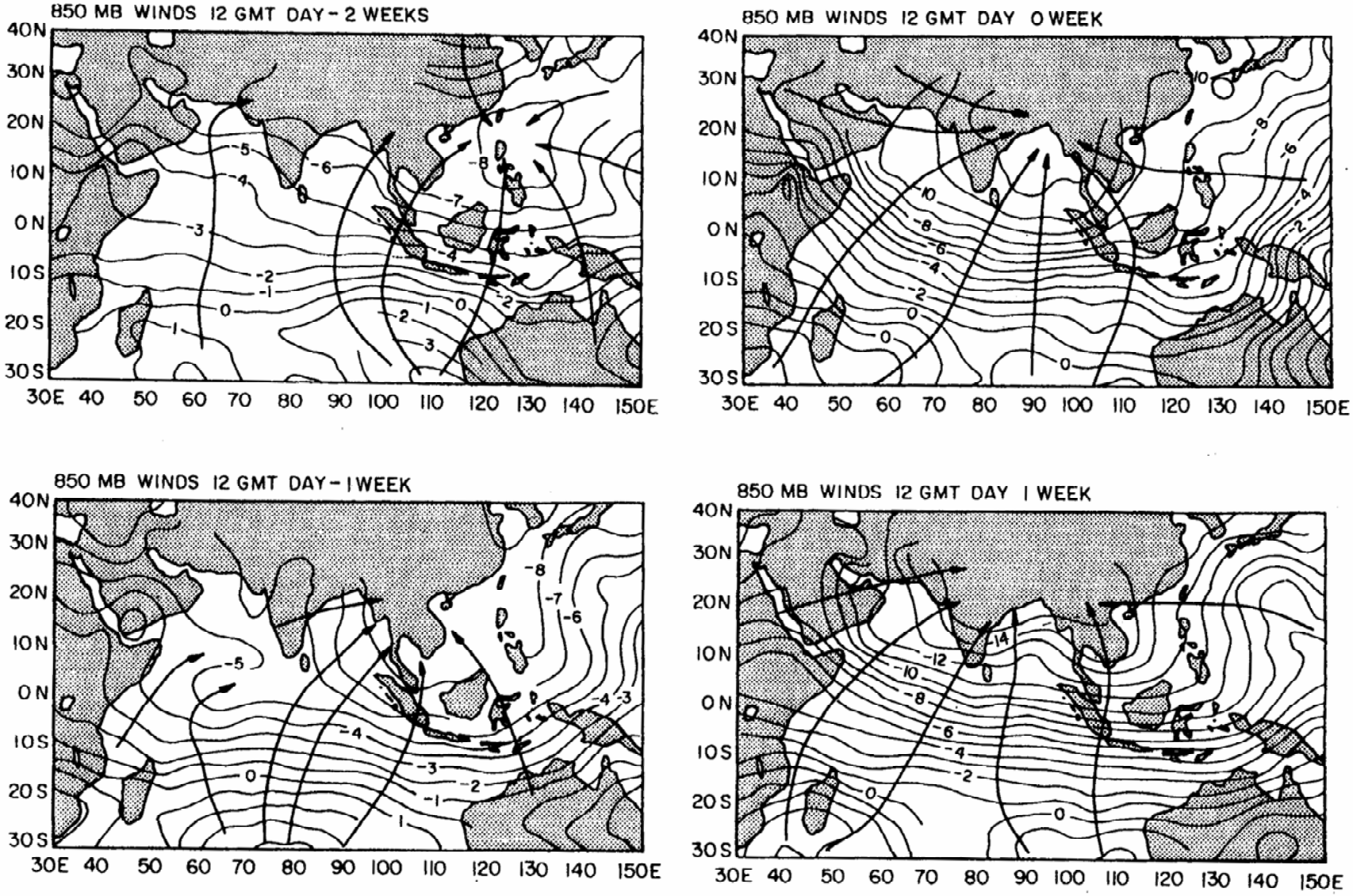

Fig. 1.5. The evolution of the velocity potential at 850 mb at two weeks prior to the onset, one week prior to the onset, the week of the onset, and one week after the onset. Selected intervals of 10^5 m^2 s^{-2} for streamlines of the divergent wind are shown by heavy lines.

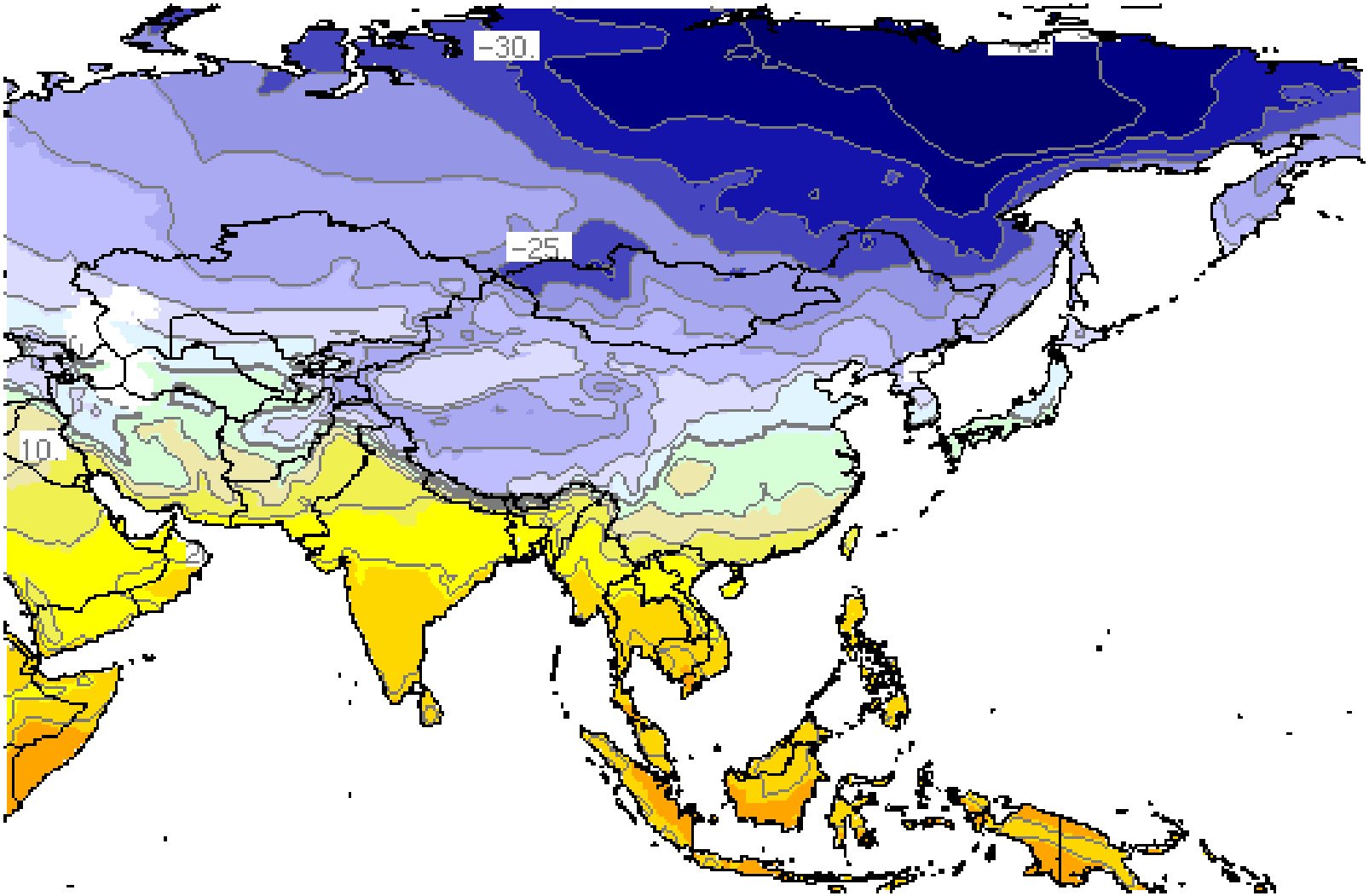

Jan

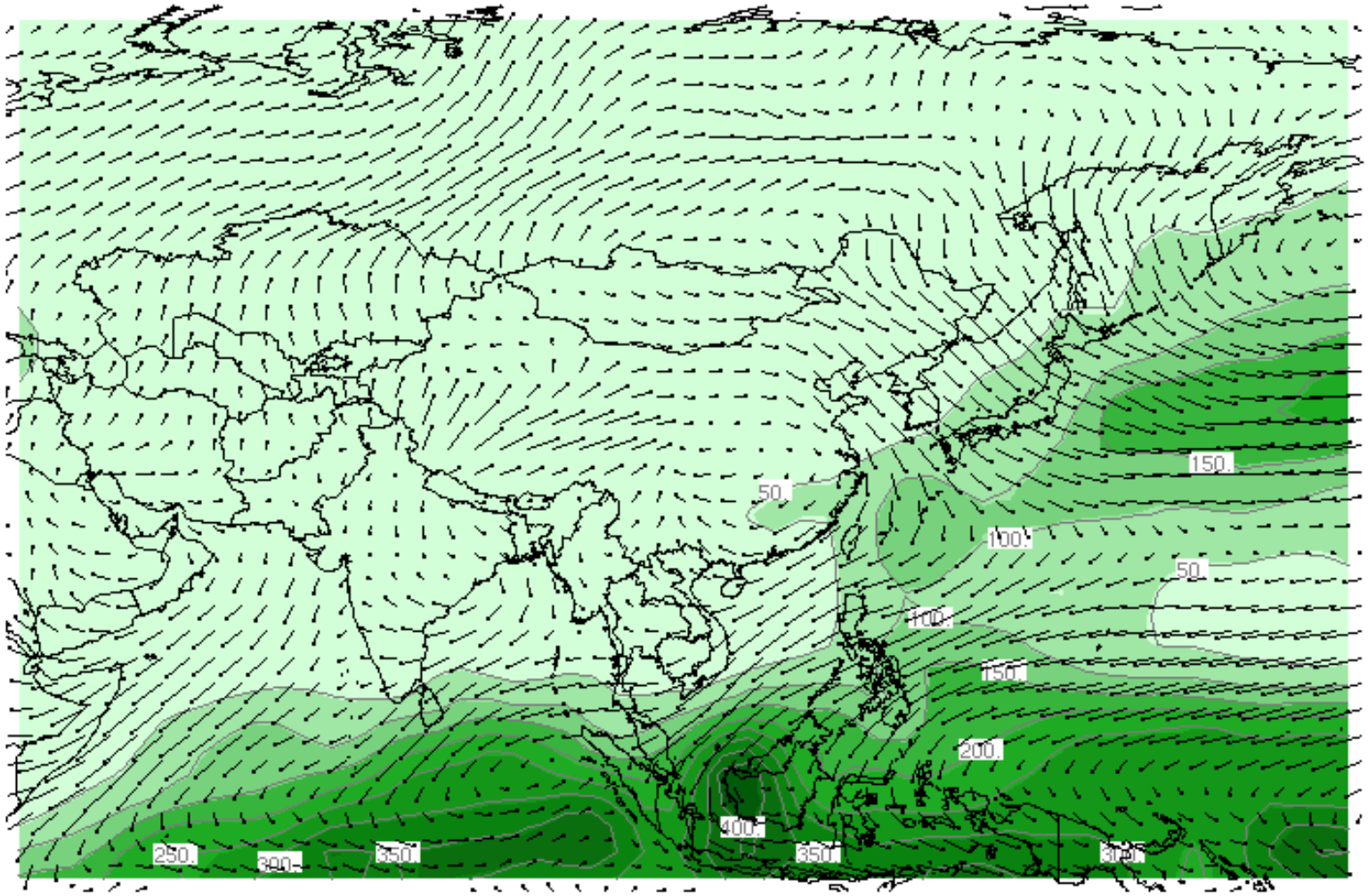

Jan 925. mb

India Monsoon Cumulative Precipitation June 1 – August 31,

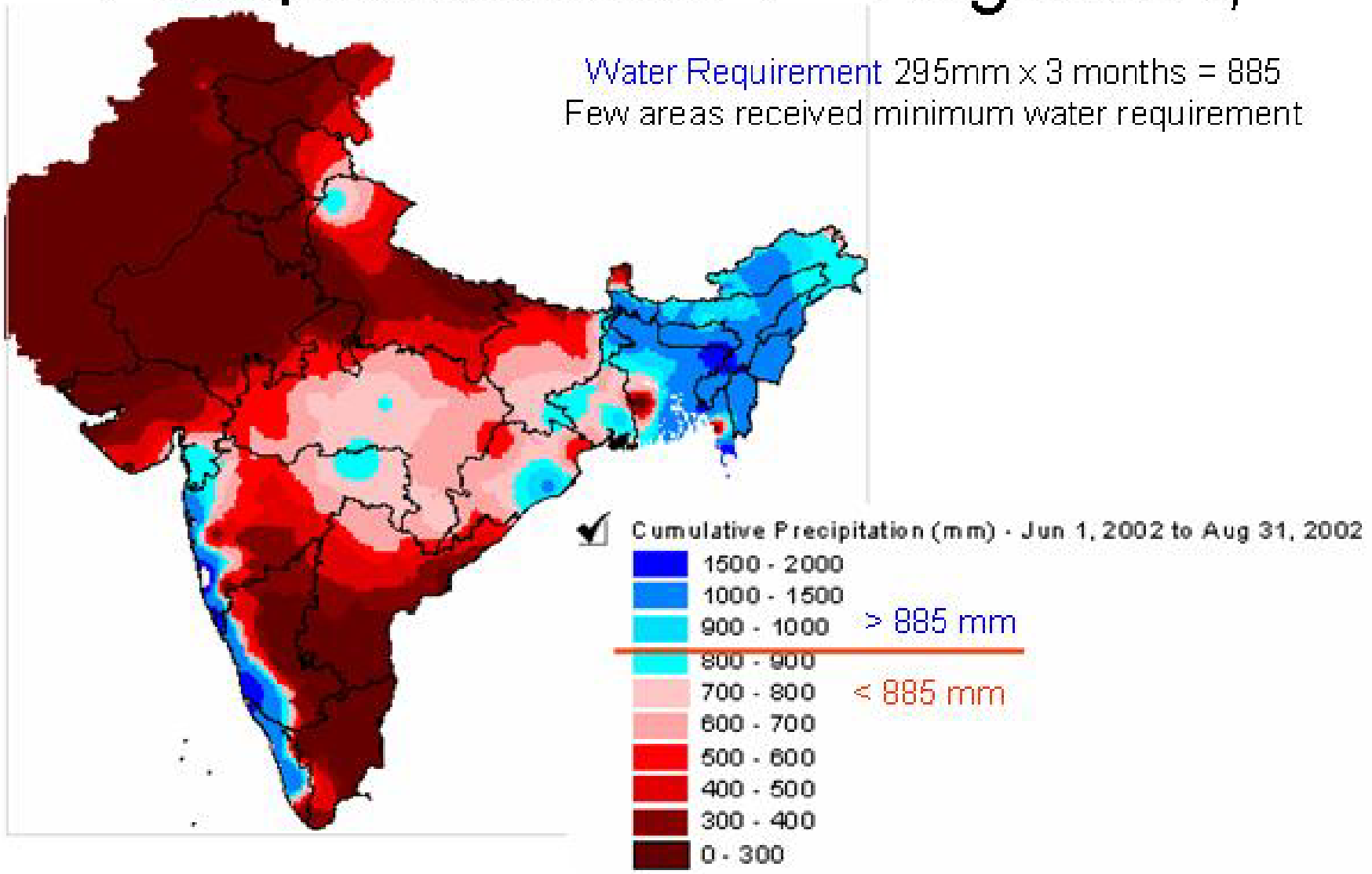

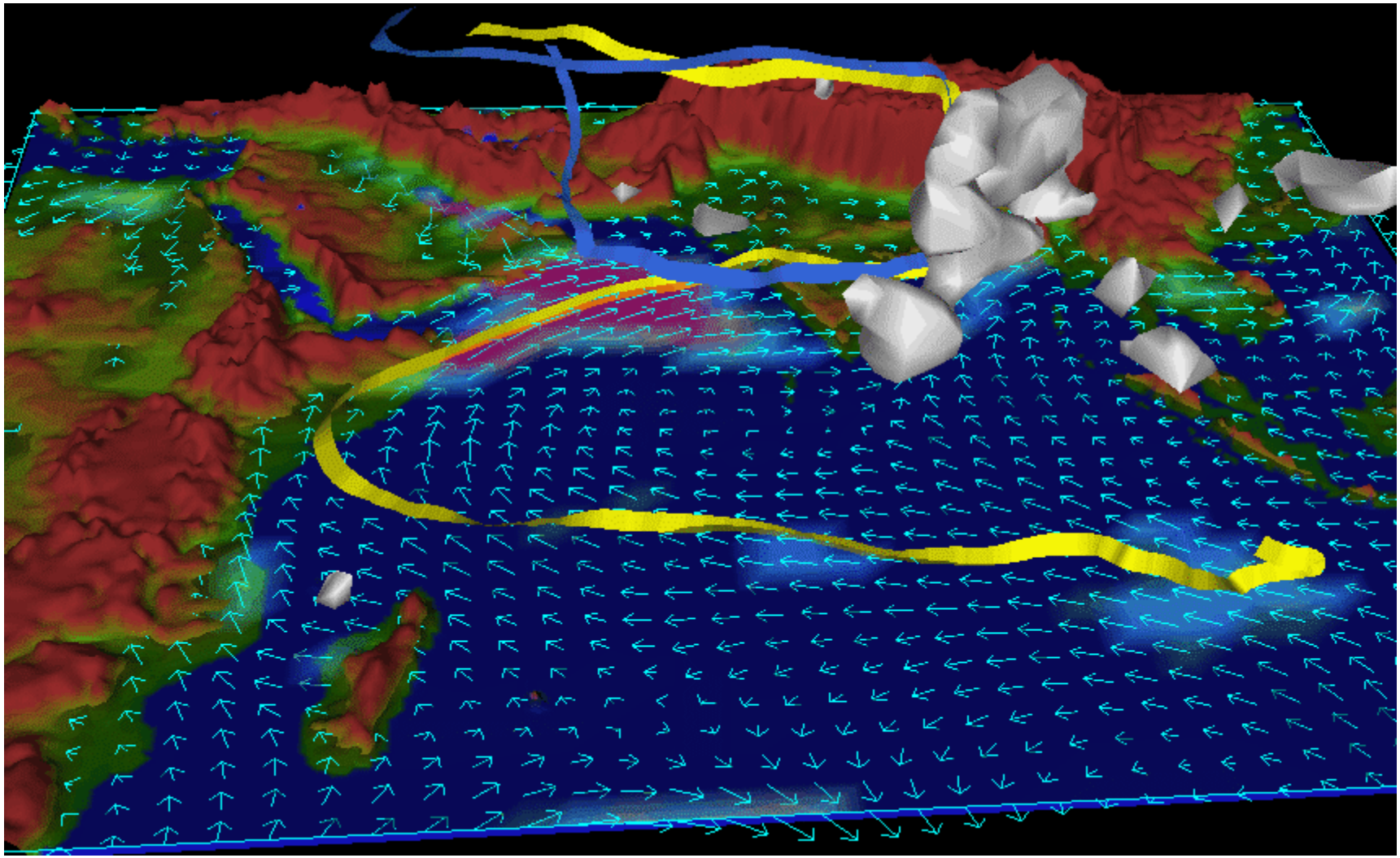

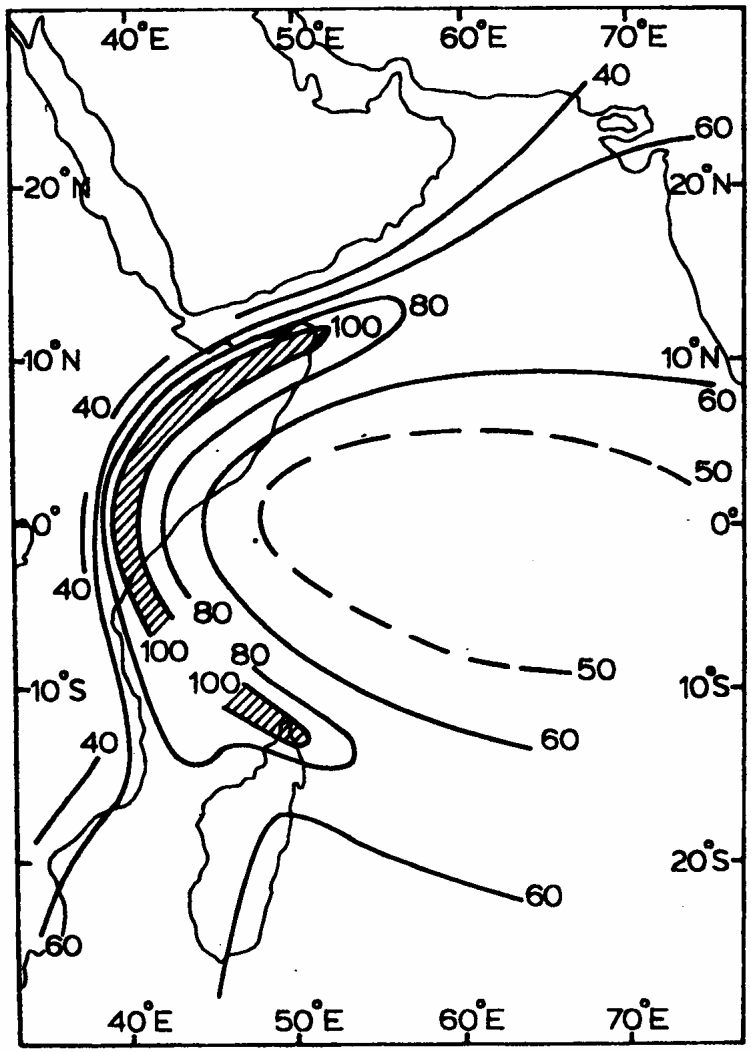

Figure 3
Smoothed isopleths of maximum wind speed (in knots) for the layer 2000–8000 ft (600–2400 m) above MSL during the period of the northern summer monsoon. 1 kt = 0.5148 ms^{-1}.

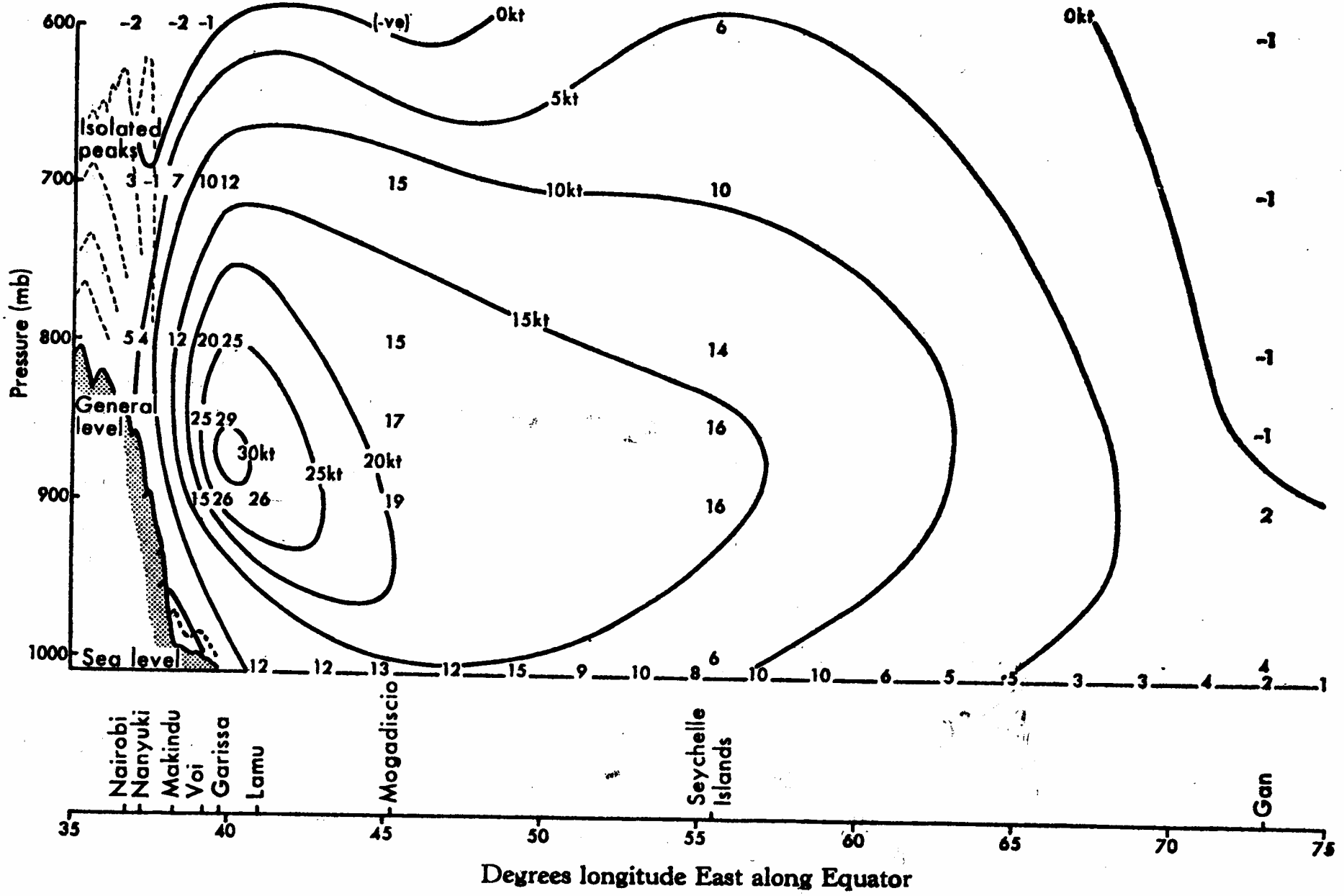

Fig. 4.1 Mean meridional flow at the Equator in July. (Findlater, 1969).

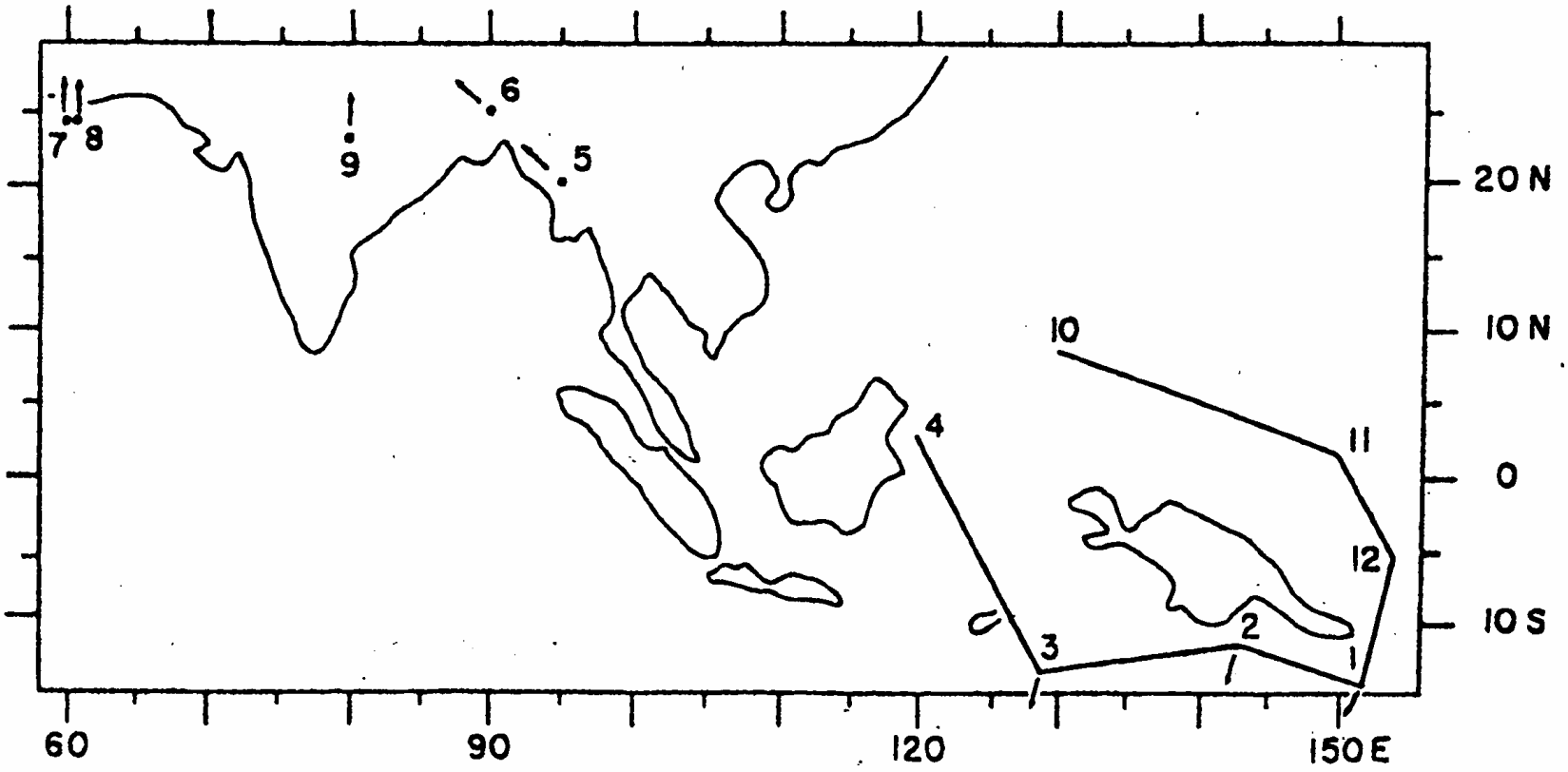

Fig. 6.8.1:2. Annual variation in the latitude and longitude position of low pressure center in the area of Indonesia and the Indian Ocean. The numbers 1 through 12 denote the calendar months. Arrows mean that the lowest pressure is found over land in indicated direction from plotted coordinates. Source: U.S. Navy (1976, 1977, 1979).

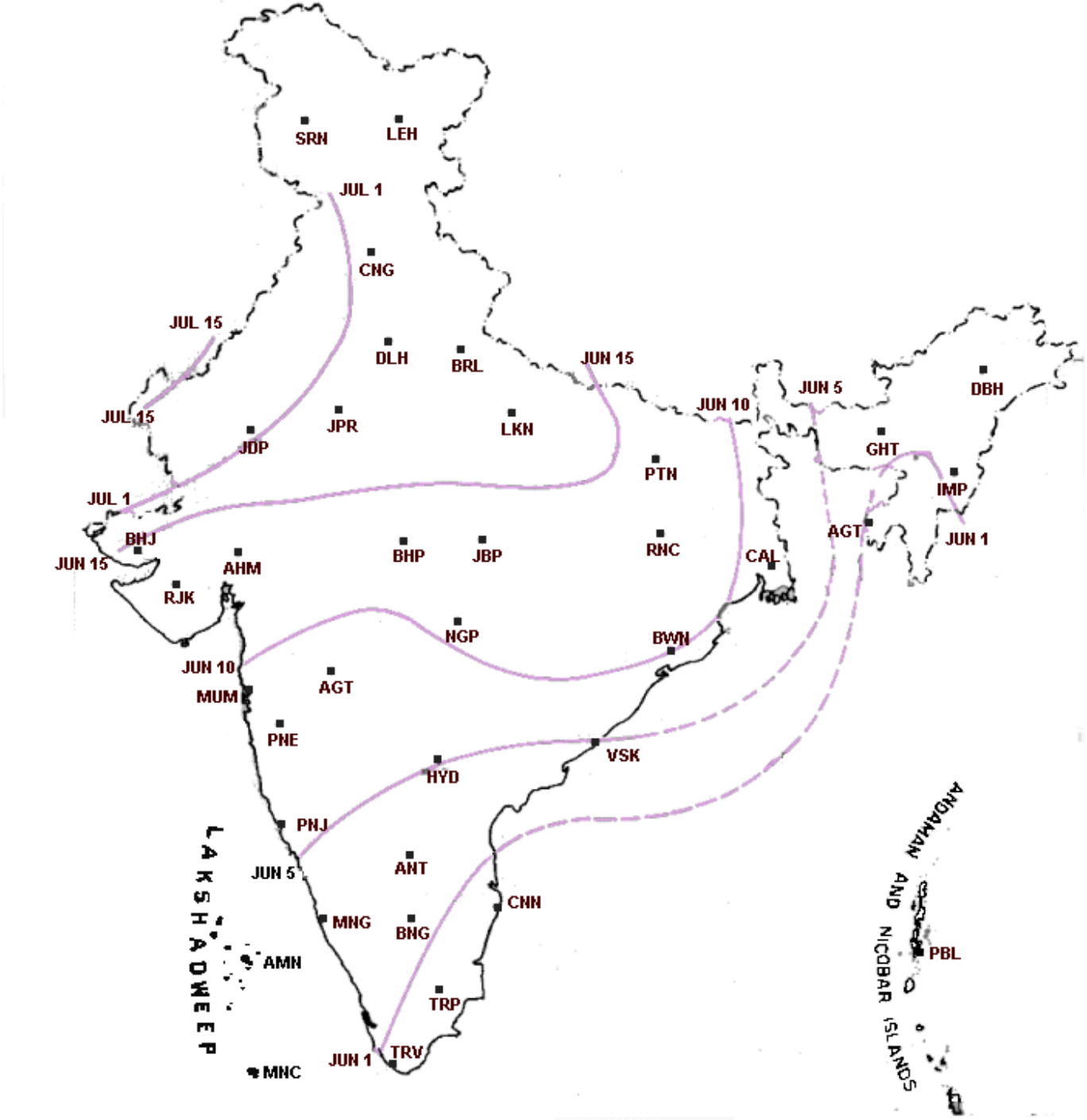
SRN
LEH
JUL 1
CNG
JUL 15
DLH
BRL
JUN 15
JUN 10
JUN 5
DBH
JUL 15
JPR
LKN
JDP
GHT
PTN
IMP
JUL 1
BHJ
AGT
JUN 1
JUN 15
AHM
BHP
JBP
RNC
CAL
RJK
NGP
BWN
JUN 10
AGT
MUM
PNE
VSK
HYD
PNJ
ANDAMAN
AND
NICOBAR ISLANDS
LAKSHADWEEP
JUN 5
ANT
CNN
MNG
BNG
PBL
AMN
TRP
JUN 1
TRV
MNC

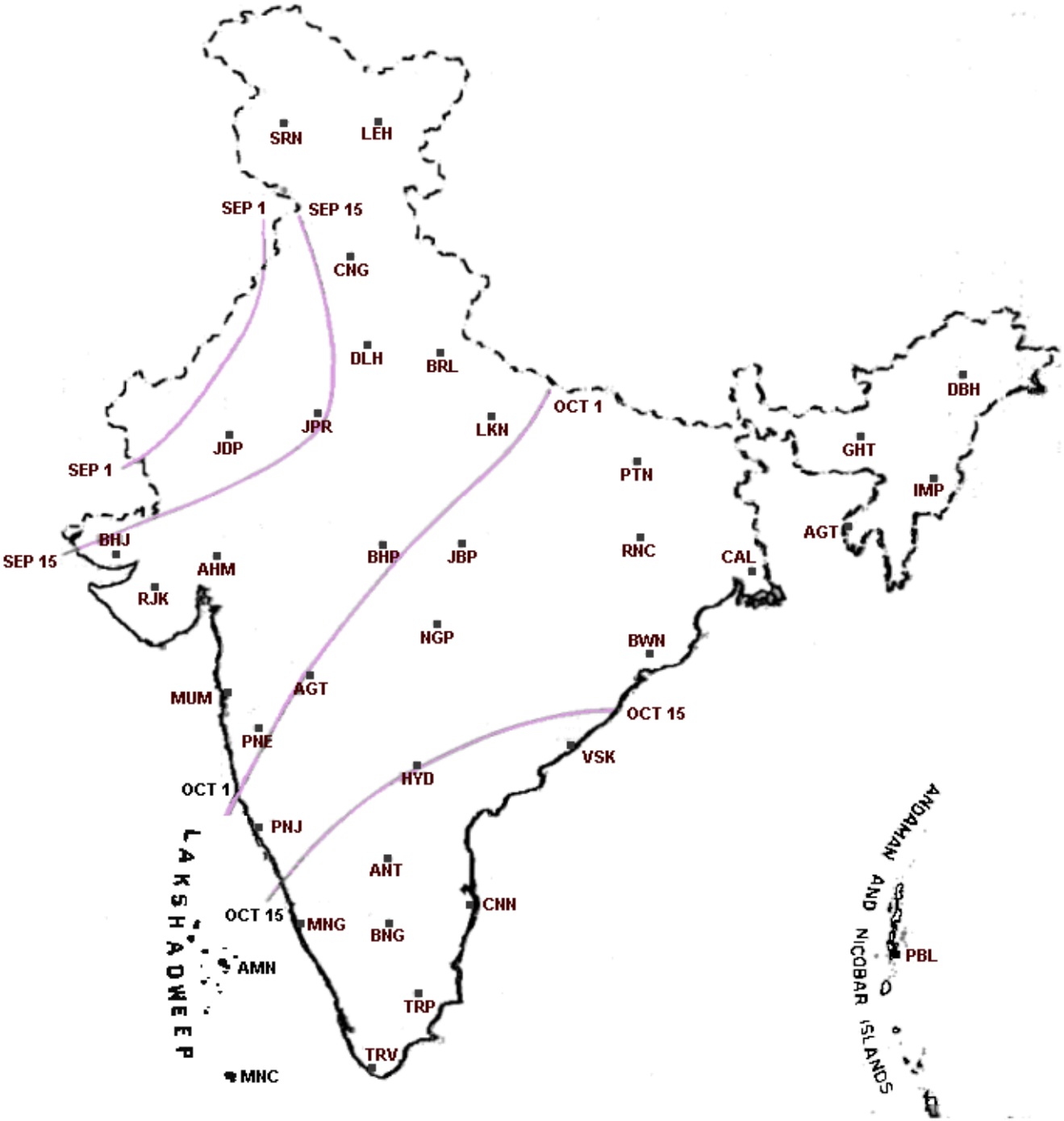
SRN
LEH
SEP 1
SEP 15
CNG
DLH
BRL
DBH
JDP
JPR
LKN
OCT 1
GHT
SEP 1
PTN
IMP
BHJ
AGT
SEP 15
AHM
BHP
JBP
RNC
CAL
RJK
NGP
BWN
AGT
MUM
OCT 15
PNE
VSK
HYD
OCT 1
PNJ
ANT
OCT 15
MNG
BNG
CNN
AMN
TRP
TRV
MNC
LAKSHADWEEP
ANDAMAN AND NICOBAR ISLANDS
PBL

NORMAL PENTAD RAINFALL
(mm)

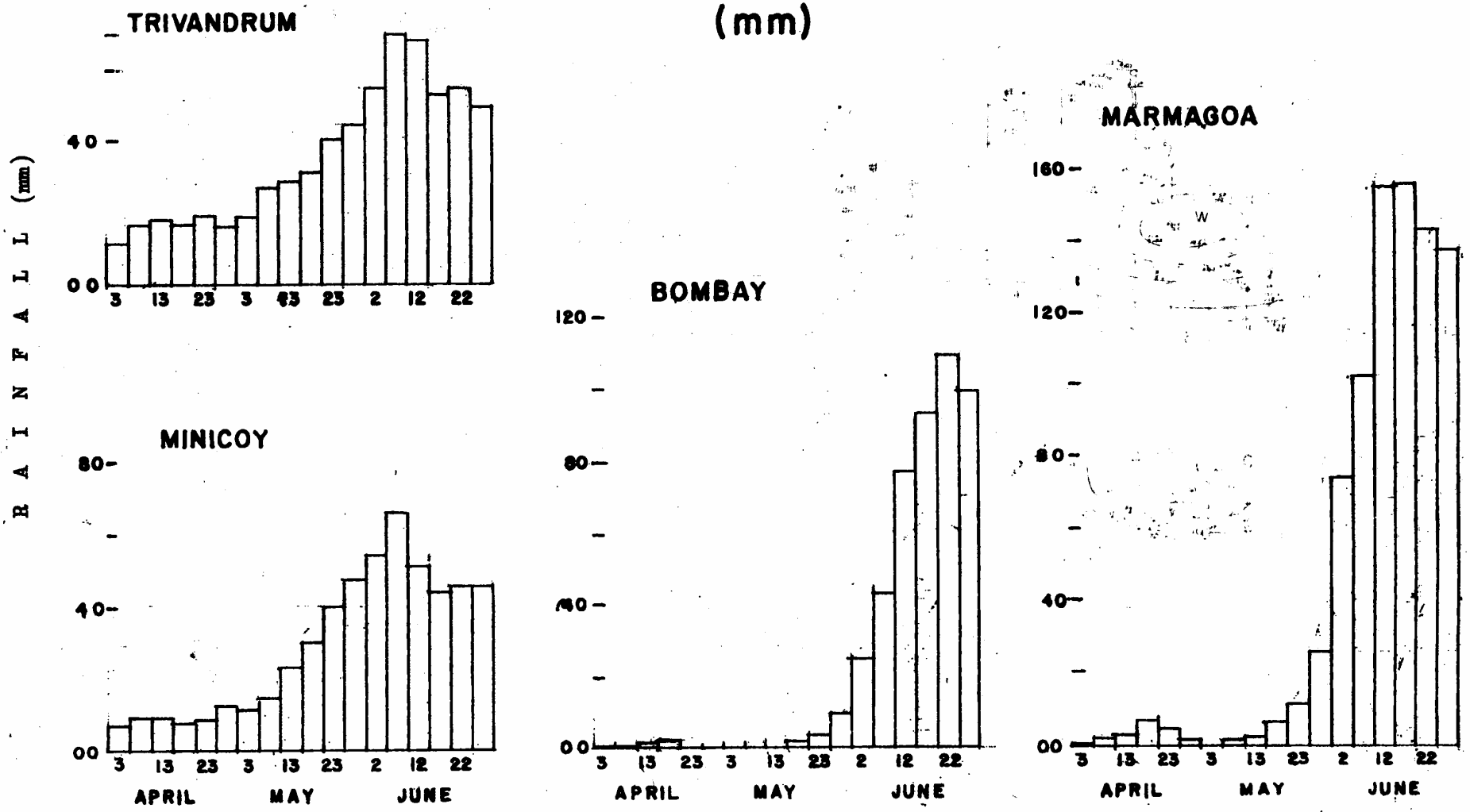

Fig. 3.2

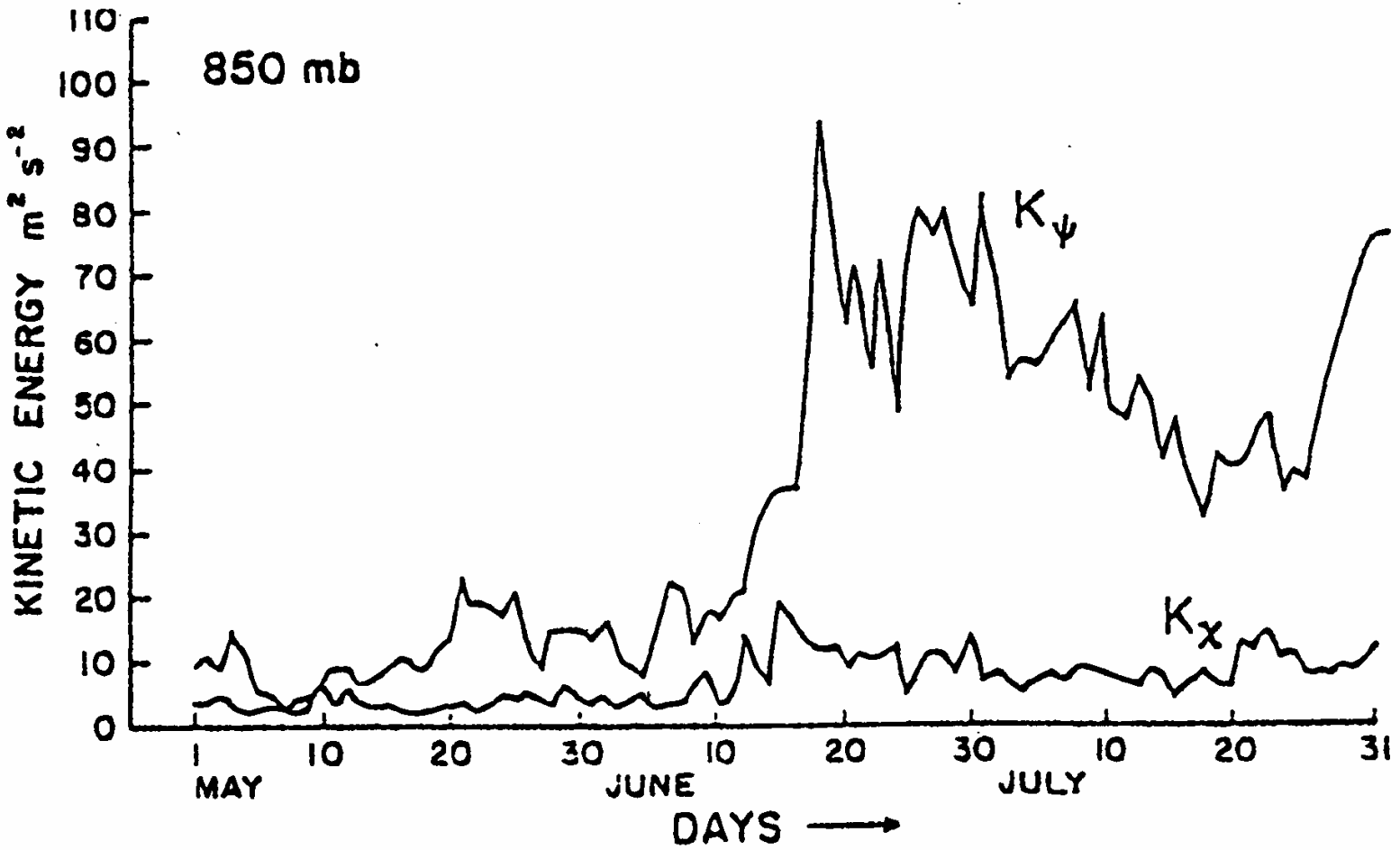

Figure 15.10. The explosive increase of winds over the Arabian Sea during the onset is seen in the time evolution of the rotational (ψ) and the divergent (χ) kinetic energy at 1.5 km above the sea level or the 850-mb level from May through June 1979. It is interesting and worth noting that the total kinetic energy (sum of K_ψ and K_χ) started to increase rapidly around June 11 over the Arabian Sea while the rainfall over central India commenced around June 18.

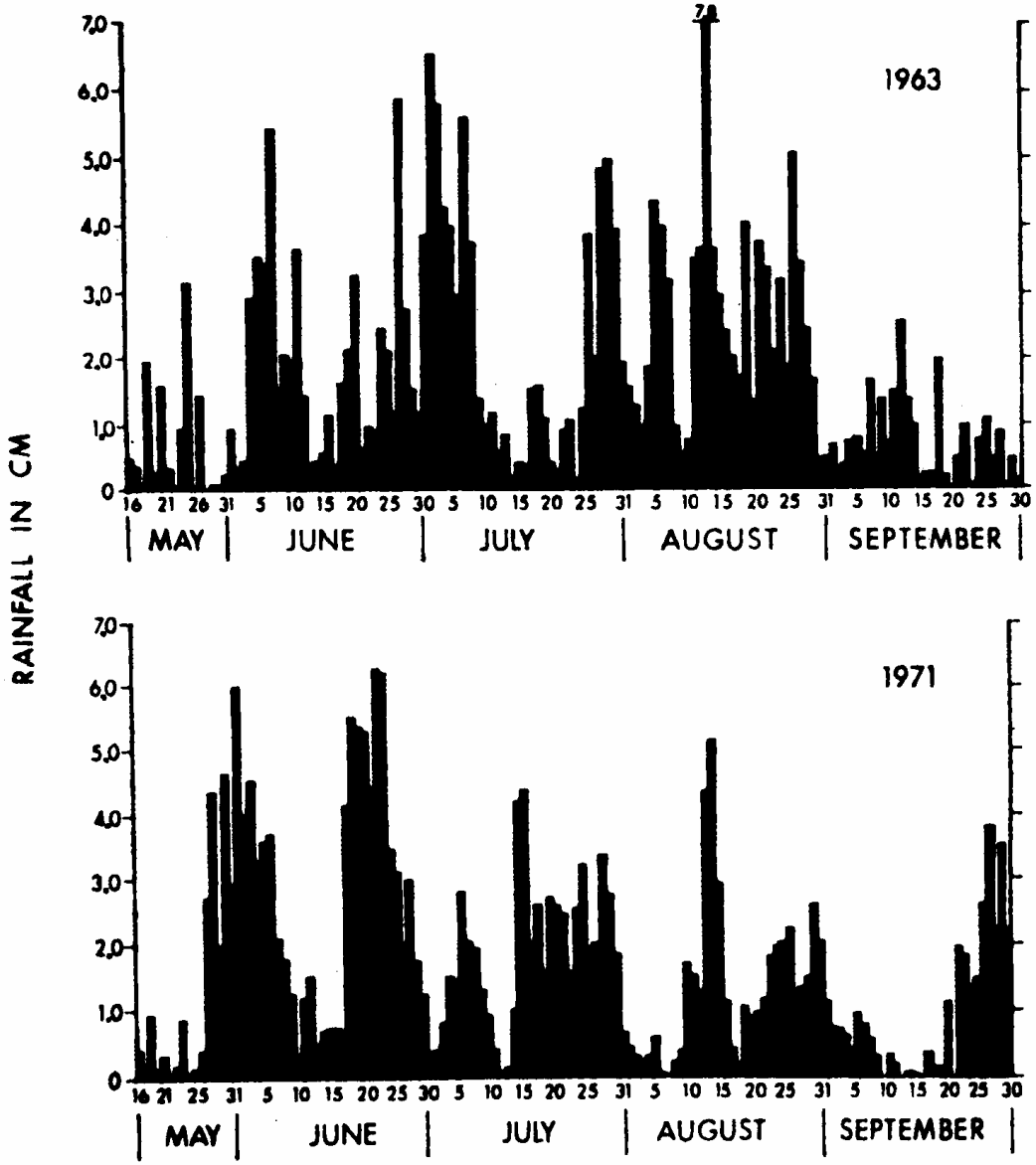

Figure 1
Daily rainfall (cm/day) along the western coast (Konkan, Coastal Mysore, and Kerala) of India during the summers of 1963 and 1971. (MURAKAMI, 1972.)

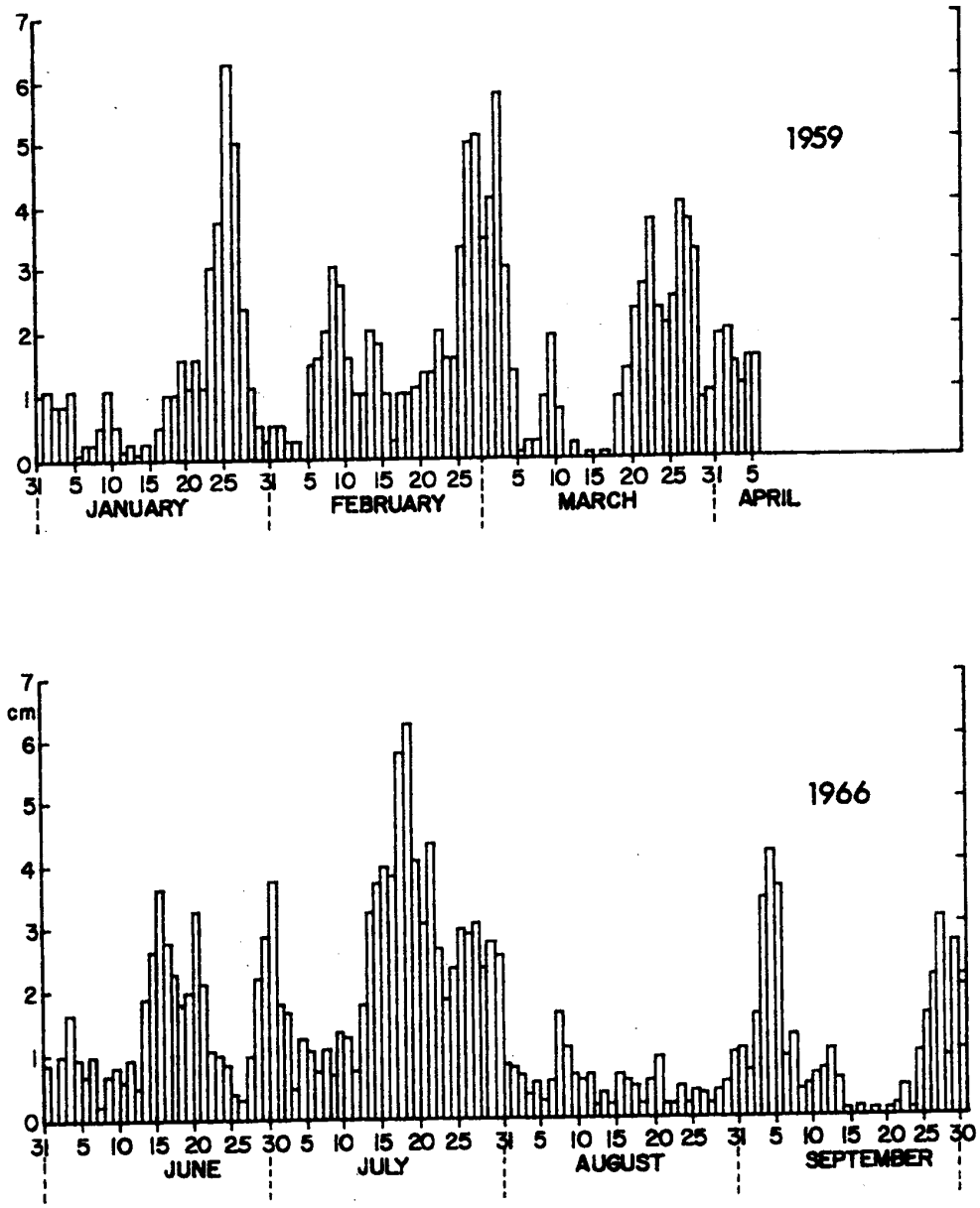

Fig. 2.8. (Top) daily rainfall "indexes" for Kenya (Johnson, 1962); abscissa, tens of percent of stations reporting rain. (Bottom) average daily rainfall along the west coast of peninsular India (Ananthakrishnan, 1966).

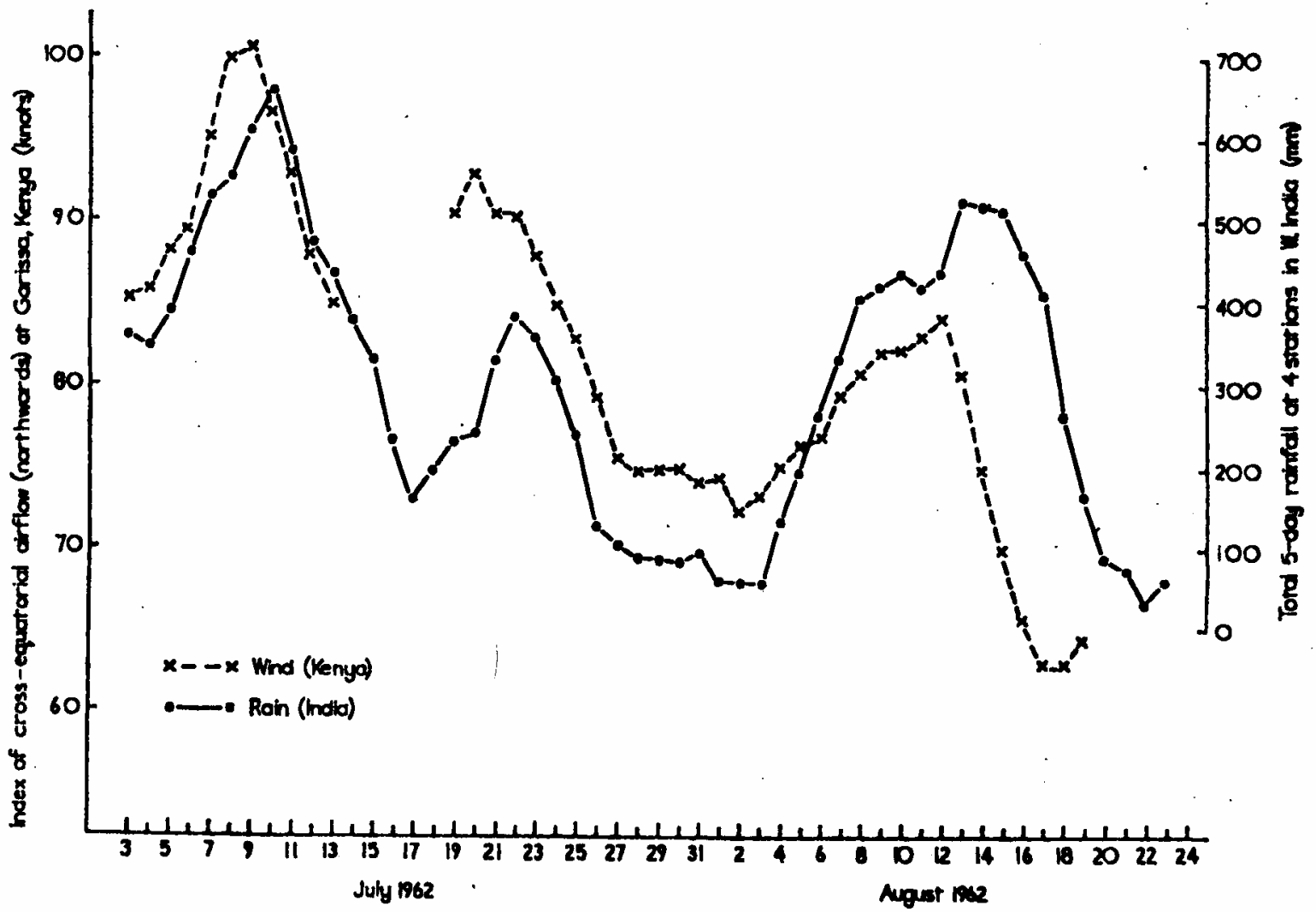

Figure 11

Cross equatorial airflow at Garissa, Kenya in relation to rainfall at four stations in western India. (FINDLATER, 1969.)

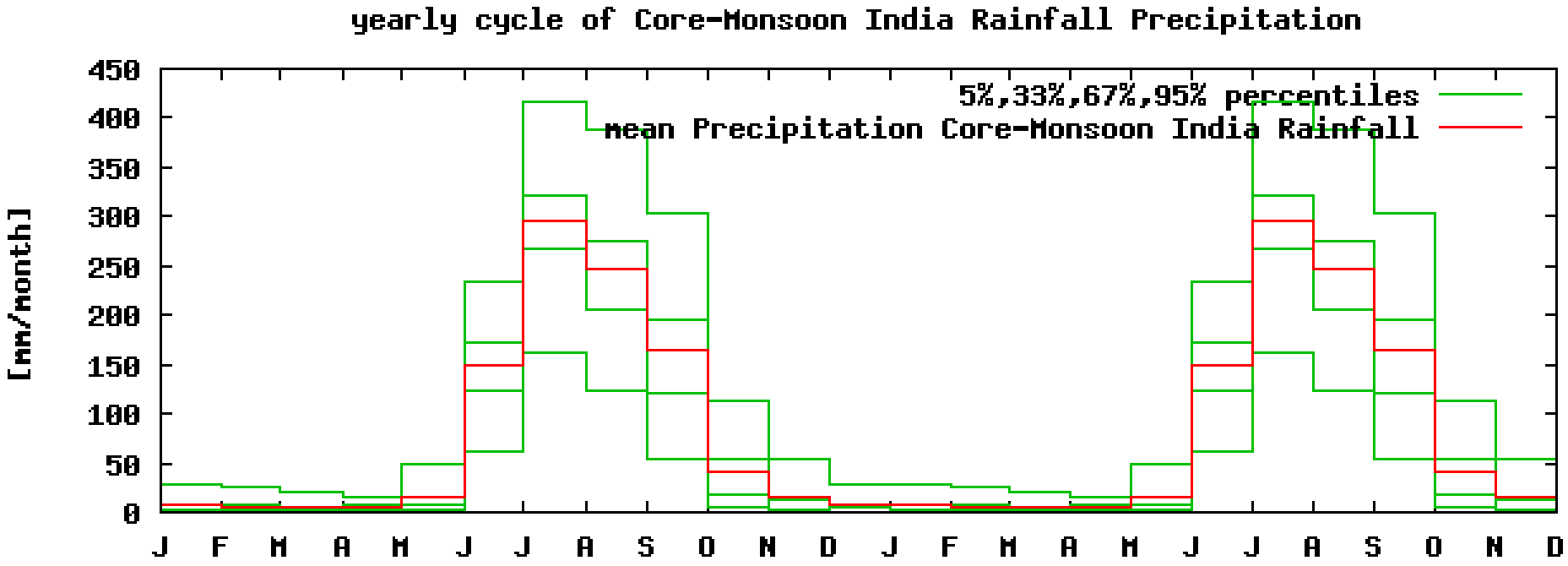
yearly cycle of Core-Monsoon India Rainfall Precipitation
[mm/month]
450
400
350
300
250
200
150
100
50
0
J F M A M J J A S O N D J F M A M J J A S O N D
5%,33%,67%,95% percentiles
mean Precipitation Core-Monsoon India Rainfall

Figure 1: Comparison of seasonal mean (June-Sept.) All India Rainfall anomalies (normalized in terms of standard deviation) from (i) observed station rain gauge record of Parthasarathy et al. (1995), (ii) satellite and surface data derived climatology of Xie and Arkin (1996), (iii) reanalysis data from ERA and NCEP/NCAR. The dashed lines represent ±1 standard deviation, typical of strong/weak monsoons.

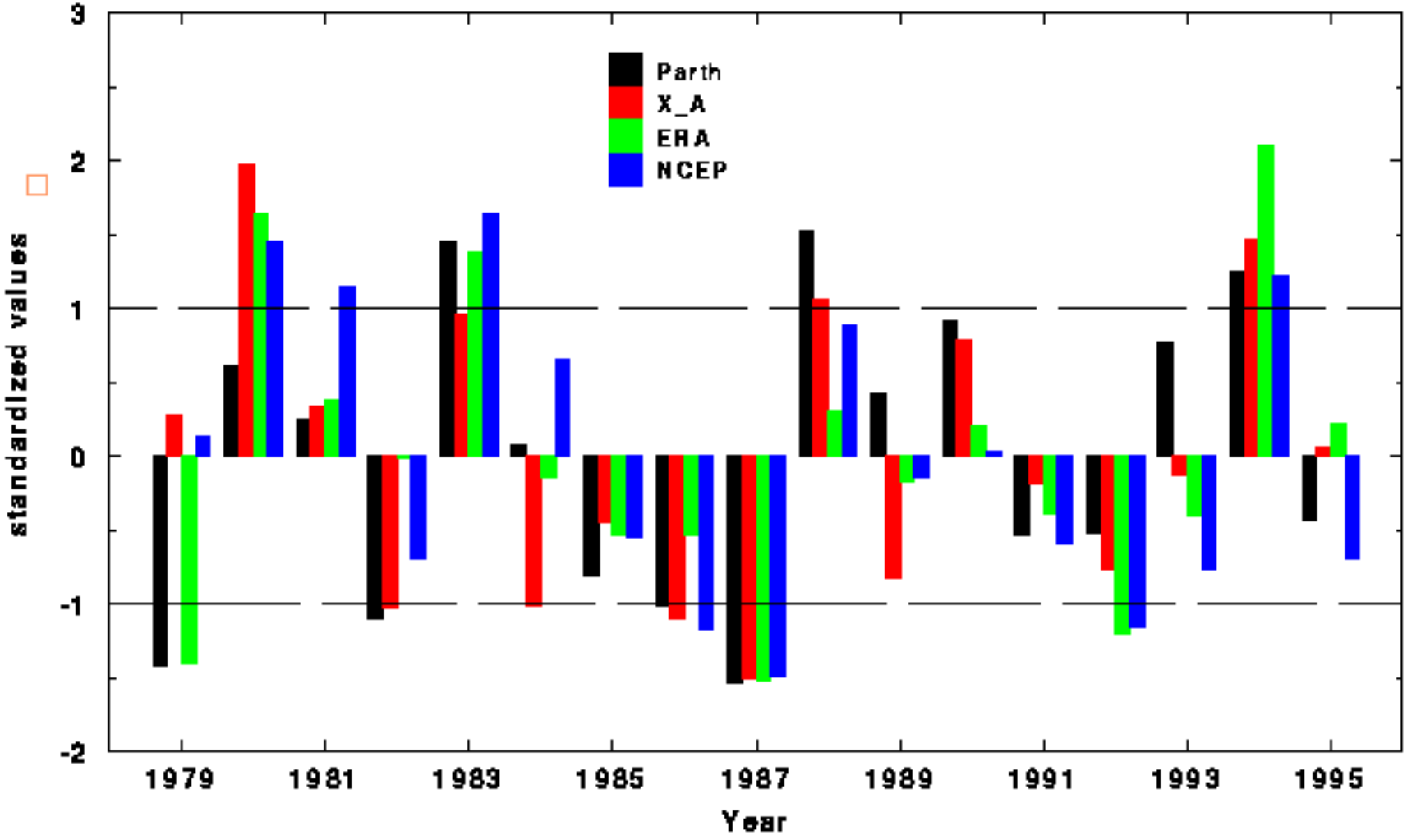

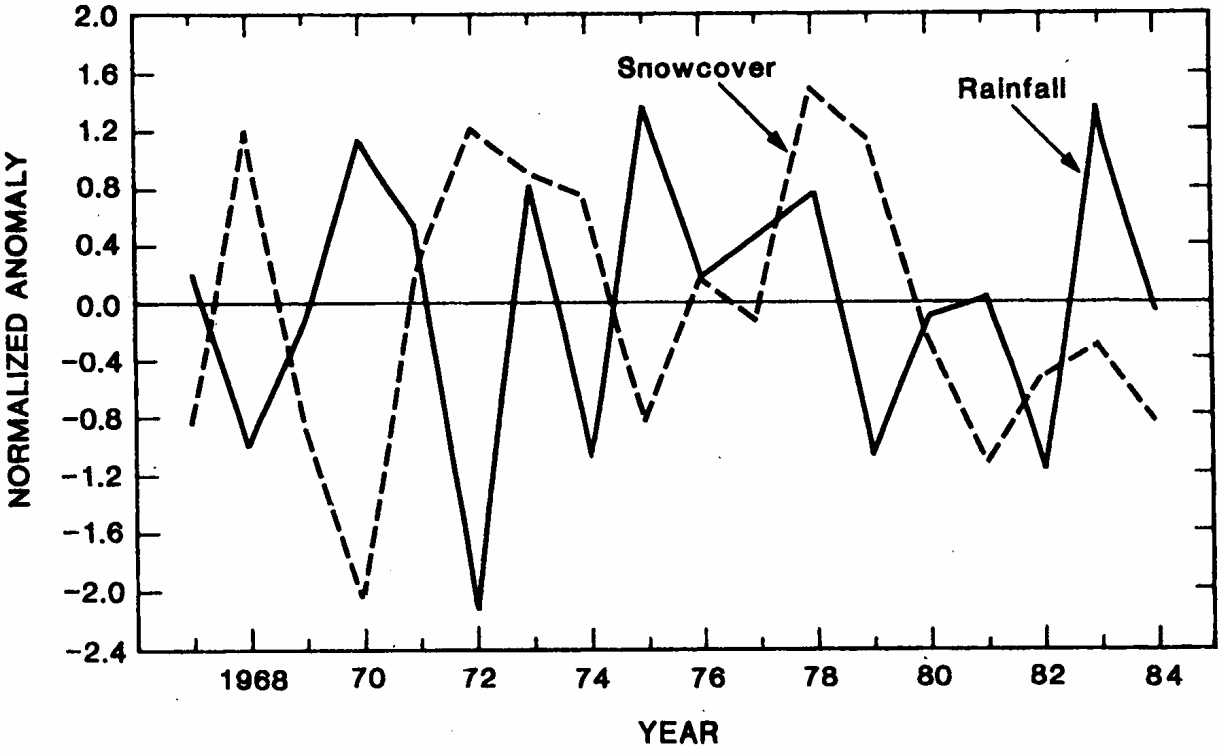

Fig. 2.18. Normalized anomaly of Indian monsoon rainfall and of Eurasian December-to-March snow cover, 1967–84.

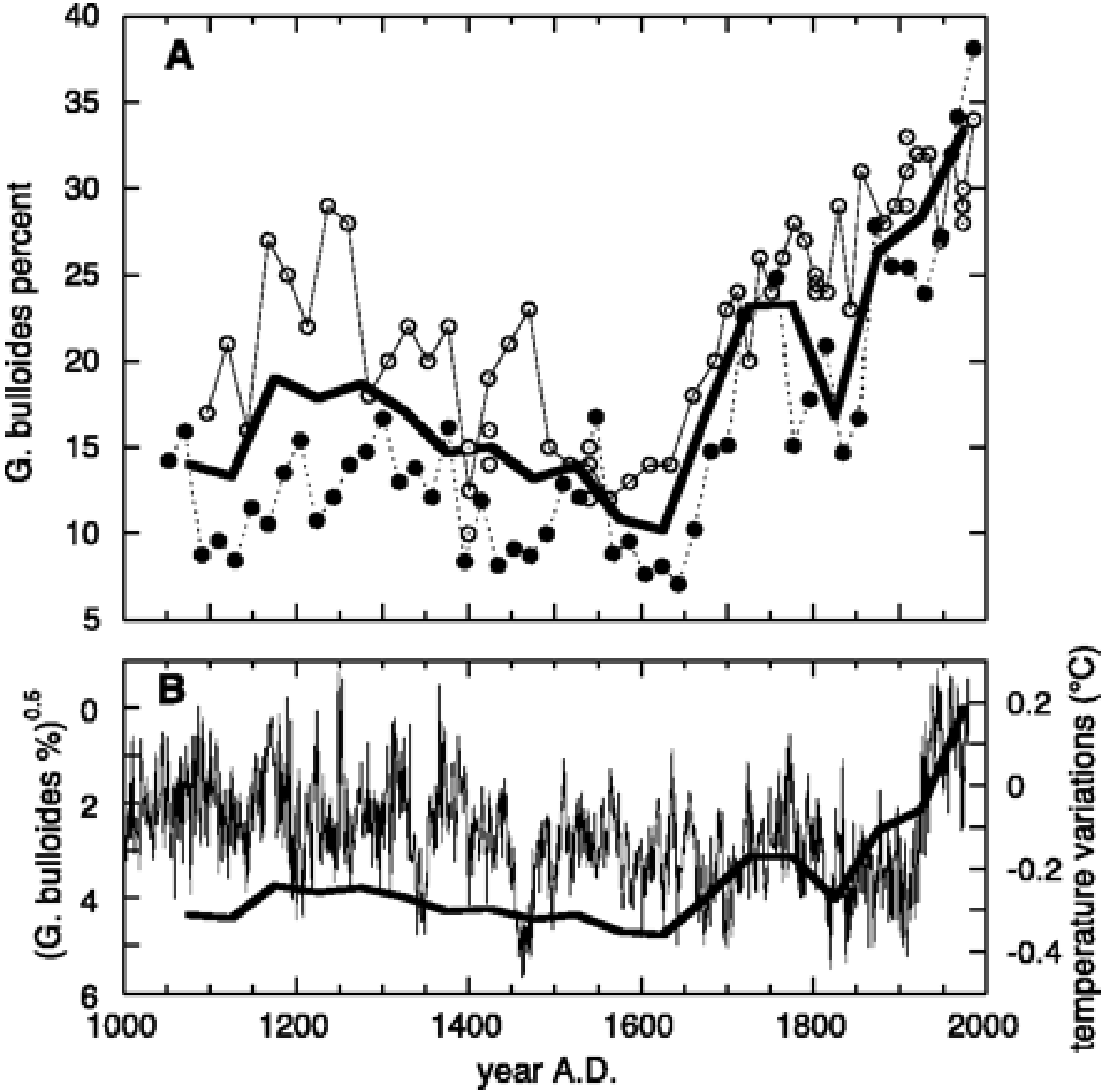
A
B
G. bulloides percent
(G. bulloides %)^0.5
temperature variations (°C)
year A.D.
40
35
30
25
20
15
10
5
0
2
4
6
0.2
0
-0.2
-0.4
1000
1200
1400
1600
1800
2000

Monsoon Depressions

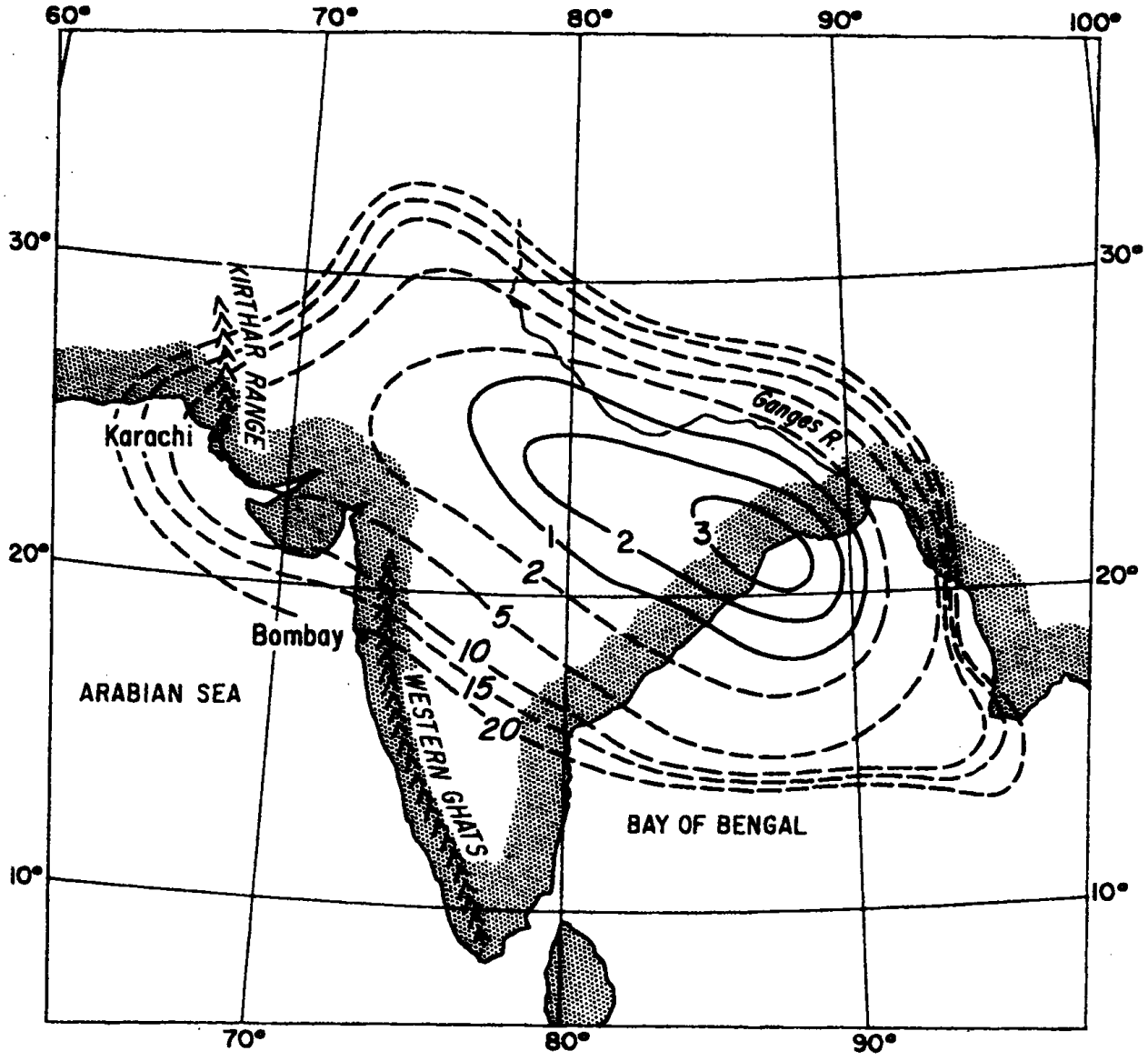

Fig. 3.19. Mean frequency of surface depression development during summer. Isopleths labeled in times per season (full lines) and in years between occurrences (dashed lines) (From Ramage, 1968a).

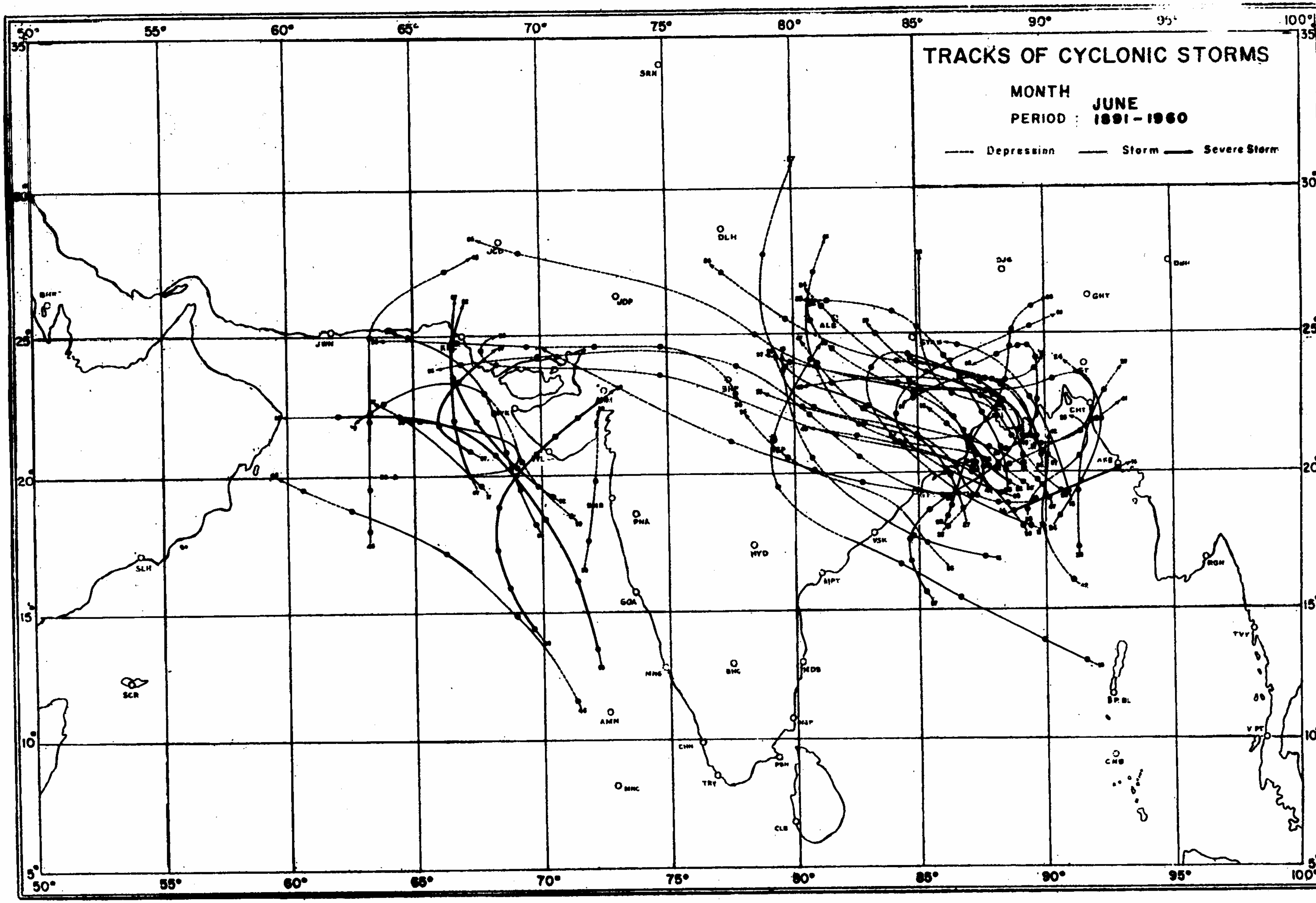
TRACKS OF CYCLONIC STORMS
MONTH JUNE
PERIOD : 1891 - 1960
Depression
Storm
Severe Storm

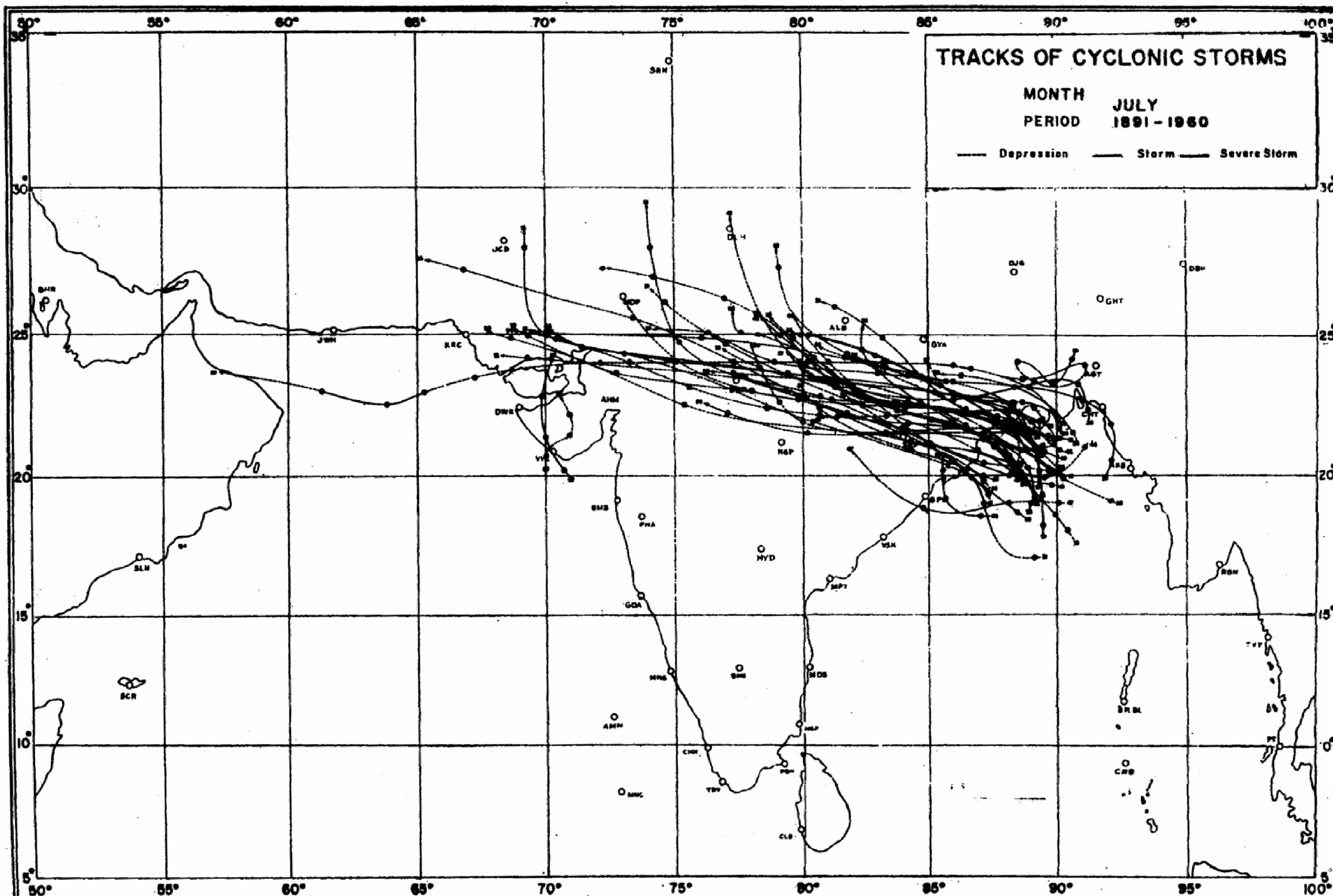
TRACKS OF CYCLONIC STORMS
MONTH JULY
PERIOD 1891 - 1960
Depression
Storm
Severe Storm

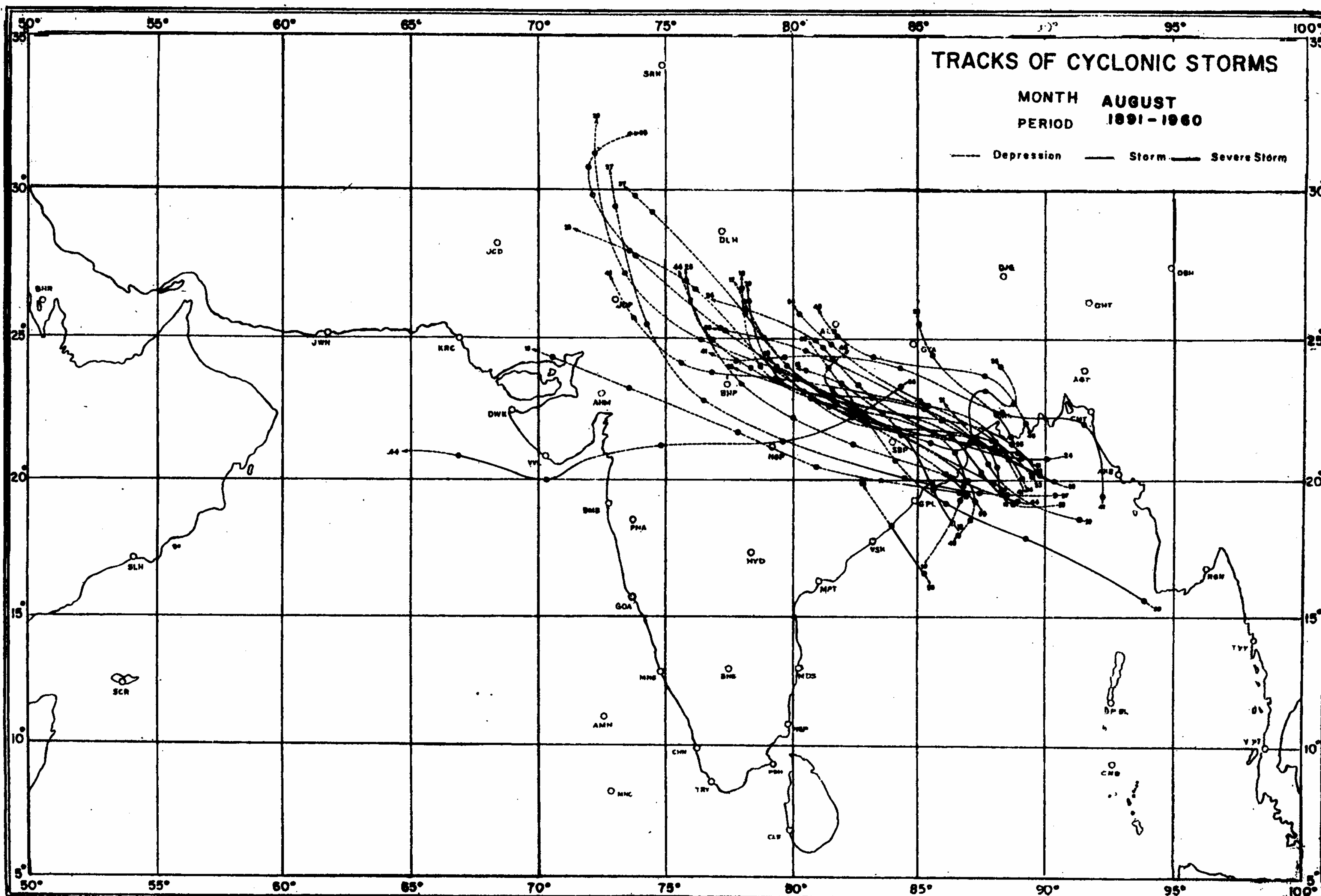

TRACKS OF CYCLONIC STORMS
MONTH AUGUST
PERIOD 1891 - 1960
Depression
Storm
Severe Storm
50°
55°
60°
65°
70°
75°
80°
85°
90°
95°
100°
35
30
25
20
15
10
5°
SRN
DLH
JCD
BHR
JWN
KRC
AHM
DWK
VVL
BHP
NGP
SBP
GYA
DJG
DBH
GHT
AGT
CHT
VSK
HYD
MPT
BMB
PNA
GOA
SLH
SCR
MNG
BNG
MDS
AMN
NGP
CHN
TRY
MNC
CLB
PBL
CNB
RGN
TVY

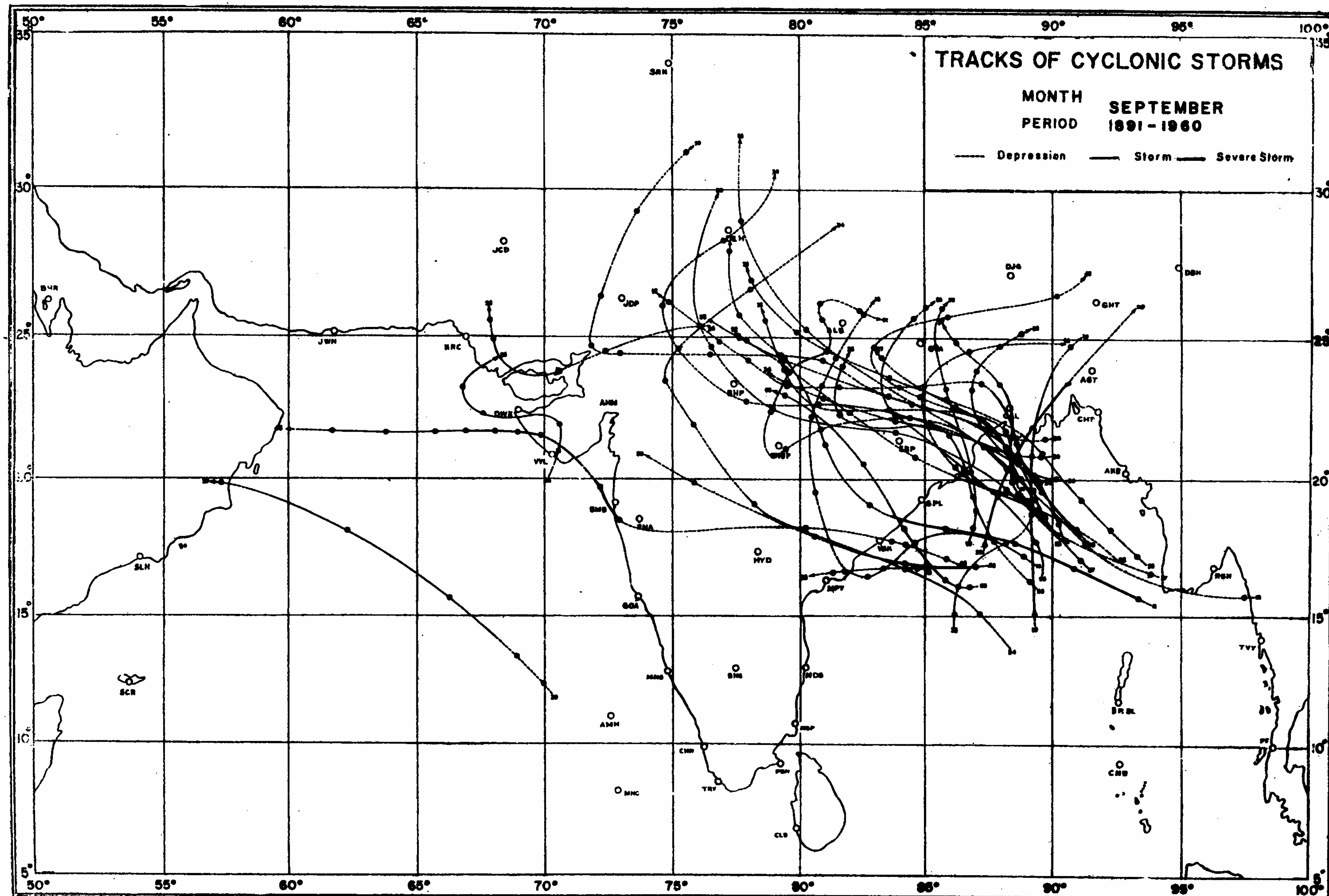
TRACKS OF CYCLONIC STORMS
MONTH SEPTEMBER
PERIOD 1891 - 1960
Depression
Storm
Severe Storm
50°
55°
60°
65°
70°
75°
80°
85°
90°
95°
100°
35
30
25
20
15
10
5°

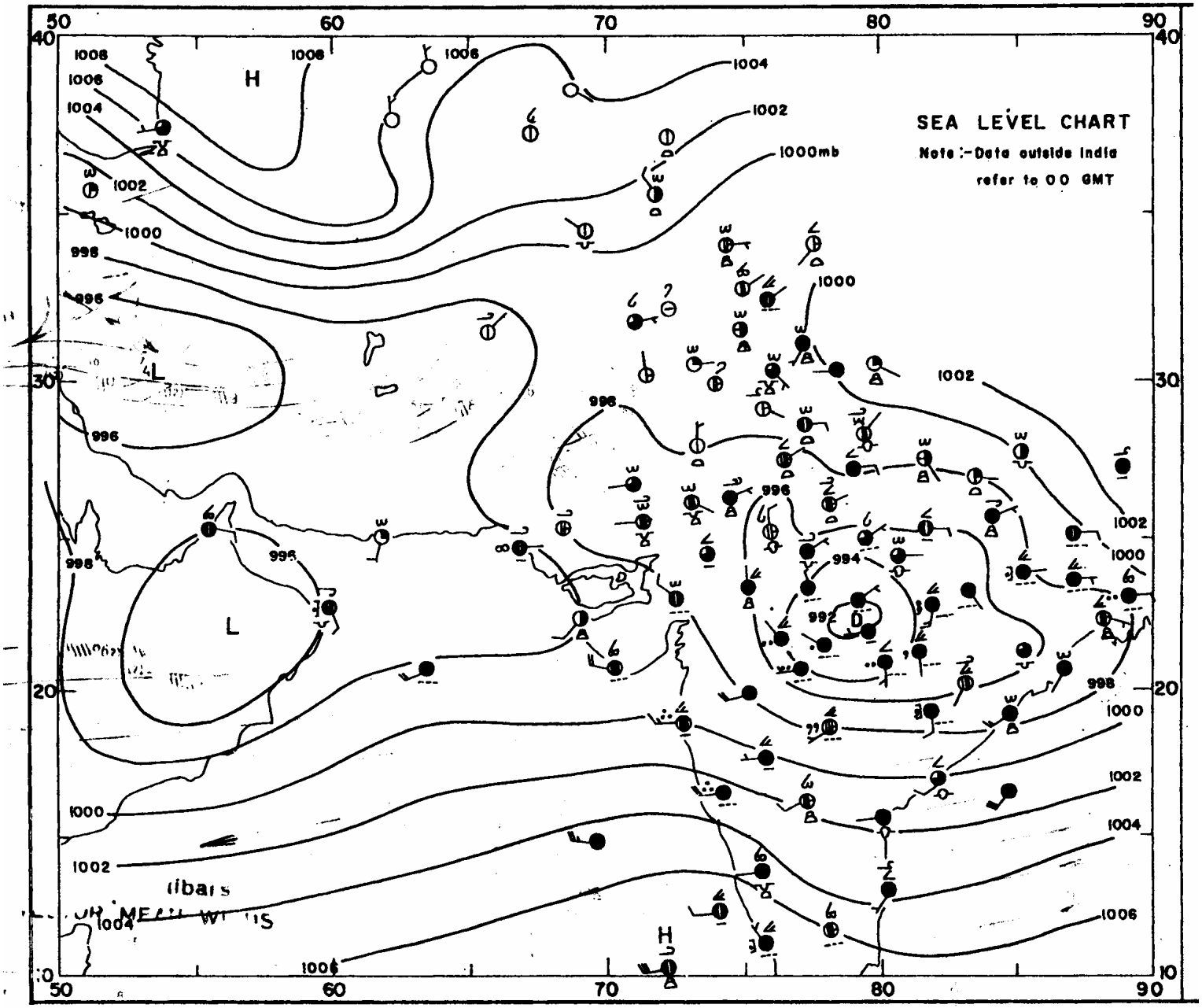

Fig.7.24(f) Synoptic charts 0300 GMT 28 July 1967

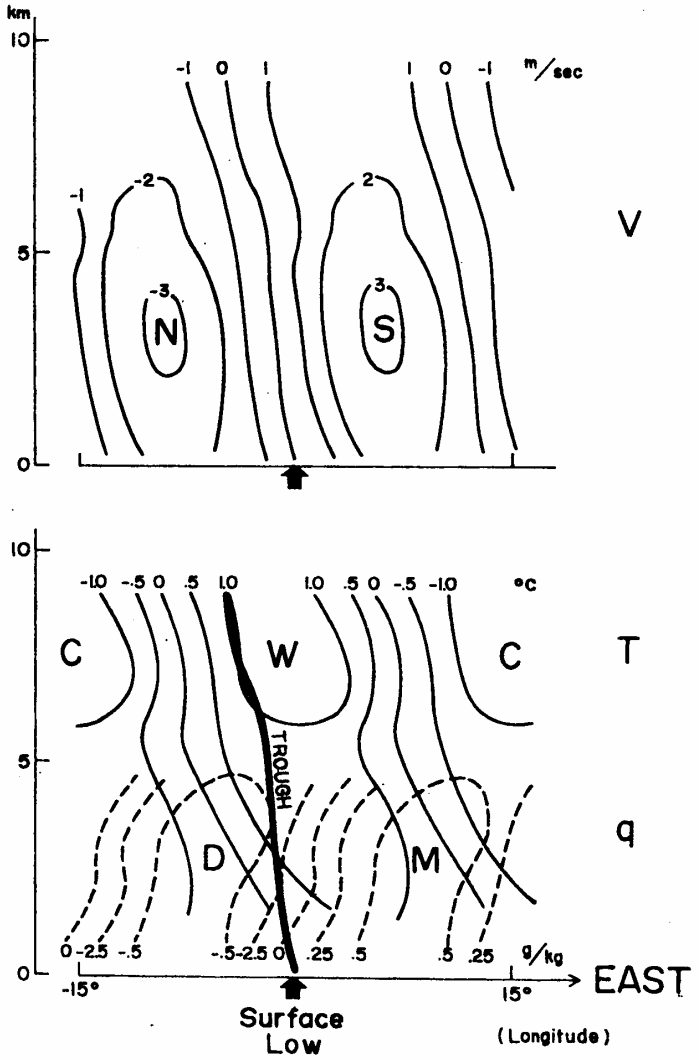

Figure 10
Mean vertical structure of monsoon lows at Calcutta. (MURAKAMI, 1976.)

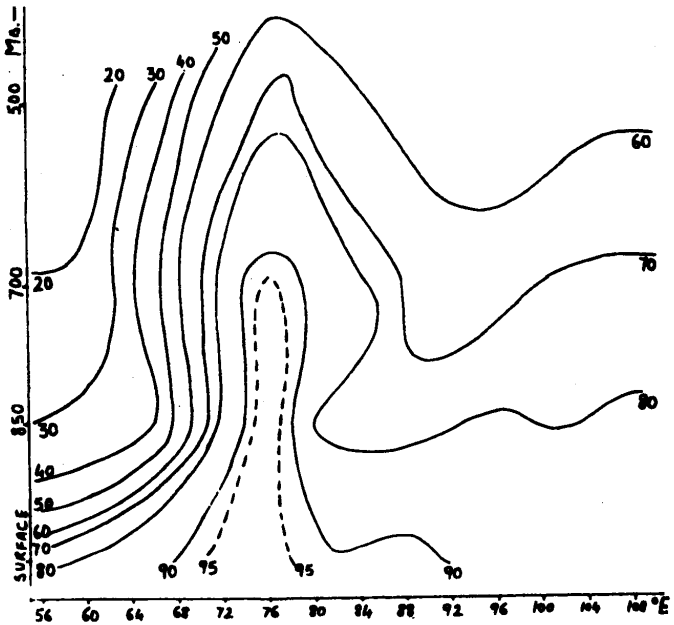

Figure 4
Vertical variation of relative humidity in the east–west direction through the centre of monsoon depression lying over western India at 00Z on 6 August, 1968 (centre of the depression 22.5°N 74.5°E).